

Testing and Optimization of Electrically Conductive Spacecraft Coatings

R.J. Mell

AZ Technology, Inc., Huntsville, Alabama

G.E. Wertz

Marshall Space Flight Center, Marshall Space Flight Center, Alabama



Prepared for Marshall Space Flight Center
under Contract NAS8-98212
and sponsored by
The Space Environments and Effects Program
managed at the Marshall Space Flight Center

The NASA STI Program Office...in Profile

Since its founding, NASA has been dedicated to the advancement of aeronautics and space science. The NASA Scientific and Technical Information (STI) Program Office plays a key part in helping NASA maintain this important role.

The NASA STI Program Office is operated by Langley Research Center, the lead center for NASA's scientific and technical information. The NASA STI Program Office provides access to the NASA STI Database, the largest collection of aeronautical and space science STI in the world. The Program Office is also NASA's institutional mechanism for disseminating the results of its research and development activities. These results are published by NASA in the NASA STI Report Series, which includes the following report types:

- **TECHNICAL PUBLICATION.** Reports of completed research or a major significant phase of research that present the results of NASA programs and include extensive data or theoretical analysis. Includes compilations of significant scientific and technical data and information deemed to be of continuing reference value. NASA's counterpart of peer-reviewed formal professional papers but has less stringent limitations on manuscript length and extent of graphic presentations.
- **TECHNICAL MEMORANDUM.** Scientific and technical findings that are preliminary or of specialized interest, e.g., quick release reports, working papers, and bibliographies that contain minimal annotation. Does not contain extensive analysis.
- **CONTRACTOR REPORT.** Scientific and technical findings by NASA-sponsored contractors and grantees.

- **CONFERENCE PUBLICATION.** Collected papers from scientific and technical conferences, symposia, seminars, or other meetings sponsored or cosponsored by NASA.
- **SPECIAL PUBLICATION.** Scientific, technical, or historical information from NASA programs, projects, and mission, often concerned with subjects having substantial public interest.
- **TECHNICAL TRANSLATION.** English-language translations of foreign scientific and technical material pertinent to NASA's mission.

Specialized services that complement the STI Program Office's diverse offerings include creating custom thesauri, building customized databases, organizing and publishing research results...even providing videos.

For more information about the NASA STI Program Office, see the following:

- Access the NASA STI Program Home Page at [**http://www.sti.nasa.gov**](http://www.sti.nasa.gov)
- E-mail your question via the Internet to [**help@sti.nasa.gov**](mailto:help@sti.nasa.gov)
- Fax your question to the NASA Access Help Desk at (301) 621-0134
- Telephone the NASA Access Help Desk at (301) 621-0390
- Write to:
NASA Access Help Desk
NASA Center for AeroSpace Information
7121 Standard Drive
Hanover, MD 21076-1320



Testing and Optimization of Electrically Conductive Spacecraft Coatings

R.J. Mell

AZ Technology, Inc., Huntsville, Alabama

G.E. Wertz

Marshall Space Flight Center, Marshall Space Flight Center, Alabama

Prepared for Marshall Space Flight Center
under Contract NAS8–98212
and sponsored by
The Space Environments and Effects Program
managed at the Marshall Space Flight Center

National Aeronautics and
Space Administration

Marshall Space Flight Center • MSFC, Alabama 35812

NASA Center for AeroSpace Information
7121 Standard Drive
Hanover, MD 21076-1320
(301) 621-0390

Available from:

National Technical Information Service
5285 Port Royal Road
Springfield, VA 22161
(703) 487-4650

TABLE OF CONTENTS

1.0	INTRODUCTION	1
1.1	Background.....	1
1.1.1	Surface Charging.....	2
1.2	Coatings.....	2
1.3	Purpose	4
1.4	Program Objectives.....	4
2.0	RESEARCH AND EVALUATIONS.....	5
2.1	Theory and Design.....	5
2.2	The Experimental Setup and Procedures	6
2.2.1	Test Chamber and Equipment	6
2.2.2	Test Procedure	12
3.0	Test Results	16
3.1	Spectral Solar Absorptance	16
3.2	Surface Voltage	17
3.3	Conductivity	20
4.0	Electrically Conductive Ceramic Pigments	23
4.1	Evaluation of Coating Additives and Binders	23
4.2	Optimization of Electrically Conductive Ceramic Pigments	26
5.0	Conclusion.....	28

LIST OF FIGURES

Figure 1. Diagram of Conductivity Measurement System.....	6
Figure 2. Electron and Enhanced UV Sources	7
Figure 3. Spectral Output of the Enhanced UV Source	7
Figure 4. Movable Test Sample Holder	8
Figure 5. Sample Coupon.	8
Figure 6. Conductivity Test System Control & Data Acquisition	9
Figure 7. General Layout of Conductivity Test System.....	12
Figure 8. Probe in Reference Position.....	14
Figure 9. Probe in Sample #1 Position	14
Figure 10. Probe in Sample #2 Position	15
Figure 11. Coating Surface Volts Measured During Electron Beam Exposure	18
Figure 12. Coating Surface Volts Measured During Combined Electron Beam and Solar UV Exposure	18
Figure 13. Surface Voltage (greater than 2 volts) Versus Exposure Dose.....	19
Figure 14. Surface Voltage (less than 2 volts) Versus Exposure Dose.....	19
Figure 15. Conductivity Values Derived from Electron Beam Exposure Data.....	20
Figure 16. Conductivity Values Derived from Combined Electron Beam and Ultraviolet Light Exposure Data	21
Figure 17. Conductivity Versus Exposure Dose (surface voltage greater than 2 volts)	21
Figure 18. Conductivity Versus Exposure Dose (surface voltage less than 2 volts)	22
Figure 19. Transmittance of Boeing Binder Through the Solar Spectrum.....	24
Figure 20. Solar Absorptance of Potassium Silicate Binder	25
Figure 21. Solar Absorptance Zinc Oxide Pigmented Proprietary Binder.....	26
Figure 22. Synthesized Electrically Conductive Whickers	28

LIST OF TABLES

Table 1. Representative Properties for Two Types of Thermal Control Coatings	3
Table 2. Conductivity Research Equipment	11
Table 3. Pre-Exposure Test Measurements	12
Table 4. Sample Exposure Procedure	13
Table 5. Solar Absorptance Values for Pre and Post Irradiated Test Samples.....	16
Table 6. Surface Voltage Measurements.....	22
Table 7. Current Candidate Metal Atoms and Their Use in This Program.....	23
Table 8. Support Materials	27

APPENDIX A

Figure 23. Solar Absorptance of AZ-70	A-2
Figure 24. Solar Absorptance of AZ-93	A-2
Figure 25. Solar Absorptance of AZ-100	A-3
Figure 26. Solar Absorptance of RM-400	A-3
Figure 27. Solar Absorptance of AZ-1000	A-4
Figure 28. Solar Absorptance of AZ-2000	A-4
Figure 29. Solar Absorptance of AZ-2100	A-5
Figure 30. Solar Absorptance of AZX-S1	A-5
Figure 31. Solar Absorptance of AZX-SG1	A-6
Figure 32. Solar Absorptance of AZX-SG2	A-6
Figure 33. Solar Absorptance of TMJ-810	A-7
Figure 34. Solar Absorptance of TMS-800	A-7

APPENDIX B

Figure 35. Surface Voltage Measurements of AZ-70	B-2
Figure 36. Calculated conductivity values for AZ-70	B-2
Figure 37. Surface voltage measurements of AZ-93	B-3
Figure 38. Calculated conductivity values for AZ-93	B-3
Figure 39. Surface voltage Measurements of AZ-100	B-4
Figure 40. Calculated Conductivity Values for AZ-100	B-4
Figure 41. Surface Voltage Measurements of AZ-400	B-5
Figure 42. Calculated Conductivity Values for AZ-400	B-5
Figure 43. Surface Voltage Measurements of AZ-1000	B-6
Figure 44. Calculated Conductivity Values for AZ-1000	B-6
Figure 45. Surface Voltage Measurements of AZ-2000	B-7
Figure 46. Calculated Conductivity Values for AZ-2000	B-7
Figure 47. Surface Voltage Measurements of AZ-2100	B-8
Figure 48. Calculated Conductivity Values for AZ-2100	B-8
Figure 49. Surface Voltage Measurements of AZX-S1	B-9
Figure 50. Calculated Conductivity Values for AZX-S1	B-9
Figure 51. Surface Voltage Measurements of AZX-SG1	B-10
Figure 52. Calculated Conductivity for AZX-SG1	B-10
Figure 53. Surface Voltage Measurements of TMJ-810	B-11
Figure 54. Calculated Conductivity Values for TMJ-810	B-11
Figure 55. Surface Voltage Measurements of TMS-800	B-12
Figure 56. Calculated Conductivity Values for TMS-800	B-12

1.0 INTRODUCTION

This is the Final Report discussing the work done for the Space Environmental Effects (SEE) Program. It discusses test chamber design, coating research and test results on electrically conductive thermal control coatings. These thermal control coatings are being developed to have several orders of magnitude higher electrical conductivity than most available thermal control coatings. Most current coatings tend to have a range in surface resistivity from 10^{11} to 10^{13} ohms/sq.

Historically, spacecraft have had thermal control surfaces composed of dielectric materials of either polymers (paints and metalized films) or glasses (ceramic paints and optical solar reflectors). Very seldom has the thermal control surface of a spacecraft been a metal where the surface would be intrinsically electrically conductive. The poor thermal optical properties of most metals, have in most cases, stopped them from being used as a thermal control surface. Metals low infrared emittance (generally considered poor for thermal control surfaces) and/or solar absorptance, have resulted in the use of various dielectric coatings or films being applied over the substrate materials in order to obtain the required optical properties.

During the 1970's, surface charging of spacecraft began to become a concern to the industry. In the late 1980's and early 1990's, this problem became significant as electronic systems became more sensitive to electrical anomalies and spacecraft surfaces or systems were damaged through electrical arc discharges. Electrical discharges can be generated from spacecraft interaction with the electrically neutral environment. Interaction between spacecraft and environment can cause charge segregation. This has resulted in charged spacecraft surfaces in GEO and LEO orbits, depending on the external biasing of the spacecraft. Indium tin oxide has been used to alleviate surface electrical resistivity problems for many applications. However, this and similar materials are typically deposited as thin films and tend to be susceptible to damage from cracking or de-bonding when deposited onto thin or flexible dielectric polymer substrates. Such damage to the electrically conductive thin film can cause a loss of electrical conductivity and an increase in surface charging.

A contract was awarded to AZ Technology by NASA through the SEE program and monitored through the Marshall Space Flight Center for the optimization and testing of electrically conductive spacecraft coatings. The purpose of this effort was to test both white and black spacecraft coatings in vacuum and optimize these coatings to have electrical conductivity values higher than currently available thermal control coatings. In addition, these coatings are designed to be deposited onto large complex geometry surfaces with minimal difficulty or environmental impact. Optimization of these coatings with higher conductivity will be a significant step forward in materials and spacecraft technology.

1.1 Background

A significant and recurring spacecraft problem is the build-up of surface charge resulting from interaction of the spacecraft with its orbital environment of charged particle radiation or space plasma. Charging of a spacecraft surface can further be intensified as spacecraft increase in size and/or with increased power requirements. In addition, payload sensitivity to electrical noise caused by electrical discharges are increasing for many items on spacecraft. Other factors like the electrical biasing of a spacecraft power generation system can also contribute to this

problem. Space Station will be the largest and highest-powered spacecraft put into orbit. It is anticipated the structure will be driven to approximately 140V negative to the ambient plasma and will require one or more plasma contactors to maintain a near neutral surface charge.

1.1.1 Surface Charging

Basically, spacecraft surface charging results from several different kinds of charging phenomena and how the environment interacts with the various surfaces of the spacecraft. The different kinds of charging phenomena are typically the following: 1) electrons from space plasma, 2) photoelectron emissions from spacecraft surfaces, 3) ions from space plasma, 4) secondary electron emissions generated by electron impacts, and 5) secondary electron emissions from ion impacts. Charge transfer typically occurs in one of the following ways: 1) from the surrounding environment to the spacecraft, 2) from the spacecraft to the surrounding environment, or 3) between different spacecraft surfaces. The interaction of these factors is highly complex. Though interactions of spacecraft and the space environment together cause much of the charging problems, one can not neglect the interaction that can occur between different materials on or in the spacecraft as well as electronic and electrical grounding circuits which also contribute to the formation of surface charging. Even with our current level of understanding of schemes for controlling spacecraft surface charge build up, there continues a need to develop and certify greater varieties and ranges of electrically conductive thermal control coatings for flight hardware utilization.

Spacecraft surface charging is believed to be responsible for the loss or damage of a number of satellites and the production of anomalous instrument data. With the development of spacecraft like the Tethered Space Satellite (TSS) and others carrying instrument packages far more sensitive than previous systems, the problem of conducting away surface charge has become even more difficult to master. Tethered Satellite's function was to study the space plasma environment surrounding the earth. To perform this task, the exterior surface coating not only was required to act as an effective thermal control surface, but also as a good electrical conductor. Because of this electrical conductivity requirement, current state of the art thermal control coatings were evaluated based not only on their thermal optical properties but also more importantly on the coating's intrinsic electrical conductivity. Through extensive testing and a few serendipitous events, it was found from testing that the coating originally selected and applied to TSS was ineffective because of poor electrical conductivity in a vacuum. Marshall Space Flight Center developed an effective and successful coating (RM-400) to meet the needs of the short duration TSS mission. This coating had only a short-term stability of its thermal optical properties in the space environment. This electrically conductive thermal control coating only had a required thermal optical stability requirement of about two weeks of space exposure in LEO. However, what is actually needed is long-term, space stable coatings for a variety of space and potentially aircraft applications.

1.2 Coatings

Currently, only a few thermal control coatings have been produced that have the potential to dissipate surface charge build-up for specific applications or conditions. Little is known and understood of these with the possible exception of a few with solar absorptance values of (0.18

to 0.30). These coatings are produced by Space Craft Incorporated (SCI) and Jet Propulsion Laboratory (JPL) and have been tested and used on a few spacecraft. Although effective at mitigating charge buildup they required long lead times to produce and require great expertise to deposit onto a surface. In addition, current designers in many cases want coatings that have better thermal optical properties, ease of application, space environment stability, while maintaining good or having better electrical properties. Much newer coatings and films from AZ Technology, Triton, ITTRI and Boeing have limited testing and flight history. Some are just now being considered for use on flight hardware. Of the high (0.85 to 0.98) solar absorptance coatings, most are based on polymer binders and or graphite and carbon pigments that are not appropriate for all uses or orbits. Therefore, the problem of damage from electrical arcing or discharge still cause many problems for the spacecraft industry. The coatings developed under AZ Technology's research program are completely inorganic, and are comprised of soluble glasses and ceramic pigments potentially making them useful for most if not all orbits.

Each coating has its strong areas of performance. As shown in Table 1, the ceramic coating, AZ-93, has poor performance in this category which is the most critical for its intended mission. The RM-400 performs well in the areas of conductivity and thermal emittance but falls short in the category of solar absorptance (α_s), as a radiator coating, with a value of 0.49. Typically for radiator coatings a solar absorptance value of 0.25 or less is required.

Table 1. Representative Properties for Two Types of Thermal Control Coatings

MATERIAL DESIGNATION	SOLAR ABSORPTANCE α_s	THERMAL EMITTANCE ϵ_n	VACUUM ELECTRICAL RESISTIVITY $\Omega/\text{sq.}$
Conventional TC Coating AZ-93	0.15	0.91	$10^{13}\text{-}10^{14}$
Tether satellite coating RM-400	0.49	0.89	5×10^5

Extensive research has taken place over the last few years to develop a variety of spacecraft coatings with the unique property of being able to conduct surface charge to a substrate or grounding system. The ability to conduct surface charge to a safe point, while maintaining optical properties and performance, is highly advantageous in maintaining operational space based systems. Without this mechanism, surfaces of a spacecraft can accumulate charge to the point that a catastrophic electrical breakdown can occur, resulting in damage to, or failure of the spacecraft. Ultimately, use of this type of coating will help mitigate many of the concerns that NASA and the space industry still have for their space based systems. When these spacecraft coatings are found to meet stability needs, they can be used to control electrical charge build up and possibly conduct sufficient electrons for power generation from the space plasma, as was demonstrated with the TSS. The unique coatings that have been developed and studied fall into two specific categories: 1) broadband absorber (black $\alpha_s=0.94$ to 0.97), and 2) selective absorber (white $\alpha_s=0.16$ to 0.30). These coatings have controllable solar absorptance and electrical surface resistivity values over designated ranges. These coatings were developed under a program which focused on the development of constituents and coatings to meet the study goals.

1.3 Purpose

The purpose of this research program was to test and to optimize electrically conductive thermal control coatings developed under a previous program.

This project focused on simulated space environmental effects testing with the intent of using this data to help optimize the stability and initial properties of these coatings. It was originally planned to expose candidate coatings to a new test that consisted of exposing the candidate coatings (independently) to an environment of low energy charged particles (generally 10Kev electrons) and/or UV with in-vacuum electrical resistivity measurement. Then, if possible, expose these same materials to a combined environment of VUV, UV, protons, and electrons with in-vacuum optical solar absorptance measurements. Through the utilization of such testing, the understanding of these coatings' space environmental stability would provide sufficient data to determine the coatings stability. Then, if sufficiently stable, the tests would provide data needed for their acceptance by the aerospace community and their potential use on current and future space programs.

Also included, was the design, procurement, assembly, debugging, procedural and methodology maturation, of a completely new space environmental testing chamber. Also discussed are the syntheses, formulation, and deposition of semiconductor spacecraft TC coatings, and their subsequent testing on custom configured test samples. The development and production of these types of coatings will be very useful for the management of electrical charge that can accumulate on the surface of a spacecraft. Also, the developed coatings could be used for current collection, storage, and conduction in environments where metals would not be effective because of poor thermal-optical properties or material reaction with the environment.

1.4 Program Objectives

- Determine suitable reference coatings that have significant ground testing, history, and if possible flight data;
- Determine effect on reference coatings and then baseline experimental coatings when exposed to the environment of UV, low energy e^- , and vacuum) with in-vacuum electrical conductivity measurements;
- Determine from space environmental effects data if test coatings need to be modified to meet stability requirements;
- Develop and implement a plan for optimizing test coatings (if needed);
- Scale-up material volumes to be capable of effectively meeting industry needs for at least one white and black coating with the following requirements:

- Initial properties

<u>White Coating</u>	<u>Black Coating</u>
– $\alpha_s \leq 0.30$	– $\alpha_s \geq 0.85$
– $\epsilon_T \geq 0.85$	– $\epsilon_T \geq 0.85$
– Resistivity tailorable between 10^2 to 10^9 ohm/sq.	
– Contamination potential	
> Collectable Volatile Condensable Materials CVCN < 0.1%	

- Environmental stability when exposed to the space environment for one year
- > Change in solar absorptance $\Delta\alpha_s \leq 0.10$
- > Change in resistivity $\leq 1 \times 10^2$
- Mass loss $\leq 0.5\%$ when exposed to an AO fluence of 1×10^{20} atoms

2.0 RESEARCH AND EVALUATIONS

2.1 Theory and Design

The standard approach used to measure the conductivity of a material is to bring electrodes in mechanical contact with the surface of the material to be measured. The surface voltage and current measurements, made relative to the contact area, determines the surface resistivity. However, variables such as non-uniform surface structure and contact pressure can introduce error to this measurement. Therefore a more desirable approach, both for simulating the space environment and measuring conductivity, is to replace the mechanical contacts by a beam of electrons. Since sunlight also plays an important role by enhancing surface charging, a combined electron and simulated solar spectra was used in the investigation of material conductivity.

The calculation of material conductivity used is made on the assumption that the material coatings obey Ohm's law. Ohmic materials demonstrate a linear behavior between current density and the electric field. This ratio of the current density and electric field is a constant σ , which is independent of the electric field producing the current. That is,

$$\mathbf{J} = \sigma \mathbf{E},$$

Where \mathbf{J} is the current density, \mathbf{E} is the electric field and the constant of proportionality, σ , is called the conductivity of the material.

The electron irradiation of the coating produces a potential difference ΔV across the thickness, d , of the coating. The potential difference is related to the electric field through the relationship

$$\mathbf{V} = \mathbf{E}d.$$

Therefore, we can express the magnitude of the current density as

$$\mathbf{J} = \sigma \mathbf{E} = \sigma(\mathbf{V}/d).$$

Assuming the material to be uniform, the current density \mathbf{J} is defined as current per unit area,

$$\mathbf{J} \equiv \mathbf{I}/\mathbf{A}.$$

Therefore, as illustrated in Figure 1, we can express conductivity as

$$\sigma = \mathbf{I}d/\mathbf{V}\mathbf{A}.$$

Where \mathbf{I} is the current through the coating, d is the thickness of the coating, \mathbf{V} is the voltage on the surface of the coating relative to ground and \mathbf{A} is the cross-sectional area of the coating being measured.

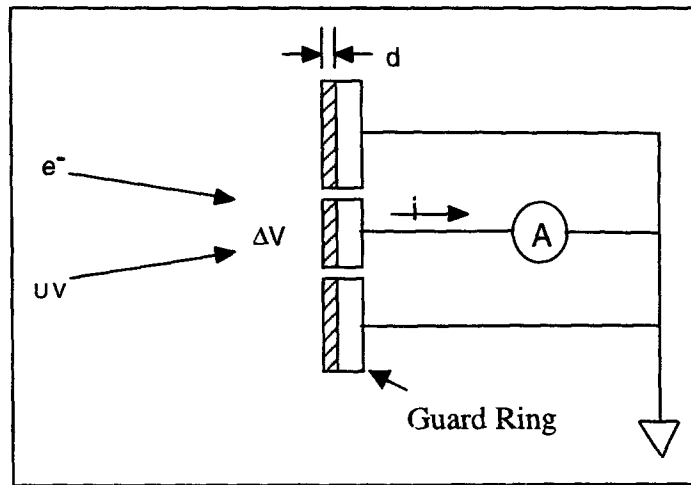


Figure 1. Diagram of Conductivity Measurement System

2.2 The Experimental Setup and Procedures

The George C. Marshall Space Flight Center designed, fabricated, and operated a unique space environmental effects test chamber incorporating the ability to measure the electrical conductivity of various spacecraft coatings. Its purpose was to record what effect different forms of energy (radiation) have on external spacecraft materials performance, function, and survivability (stability or lack of change) over time or radiation dose. As is shown and discussed in detail in the following paragraphs a custom designed vacuum chamber was fitted with both an electron flood gun and a thousand watt near ultra-violet (NUV) radiation source. These radiation sources can be used simultaneously or individually as needed to understand a particular phenomenon or material effect.

2.2.1 Test Chamber and Equipment

The test system, shown in Figure 2, consists of an energetic electron source and enhanced UV source. Each source impinges with the sample coupons at an angle of 5.5 degrees off sample normal. The test system was maintained at a base vacuum of 5×10^{-7} Torr. A Kimball Physics 50 Kev electron source was adjustable from 0 to 50 Kev and capable of generating currents up to $1\text{mA}/\text{cm}^2$. For testing purposes, the source was operated at a constant energy of 10 Kev. The electron beam current density was variable from 1 to $10\text{nA}/\text{cm}^2$.

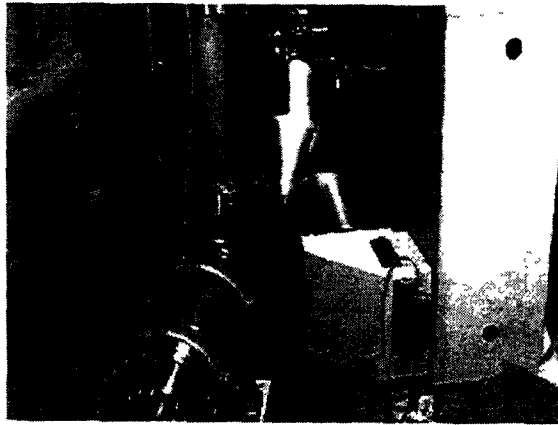


Figure 2. Electron and Enhanced UV sources

The Spectral Energy enhanced ultraviolet (UV) source uses a xenon lamp to simulate the UV output of the sun. The output of this assembly was measured with an Optronics Laboratories Model 752 Spectoradiometer. The photon flux, integrated from 200 to 400 nanometers, was measured to be $25.5 \text{ mw/cm}^2 \text{ nm}$. UV source spectral output is shown in Figure 3.

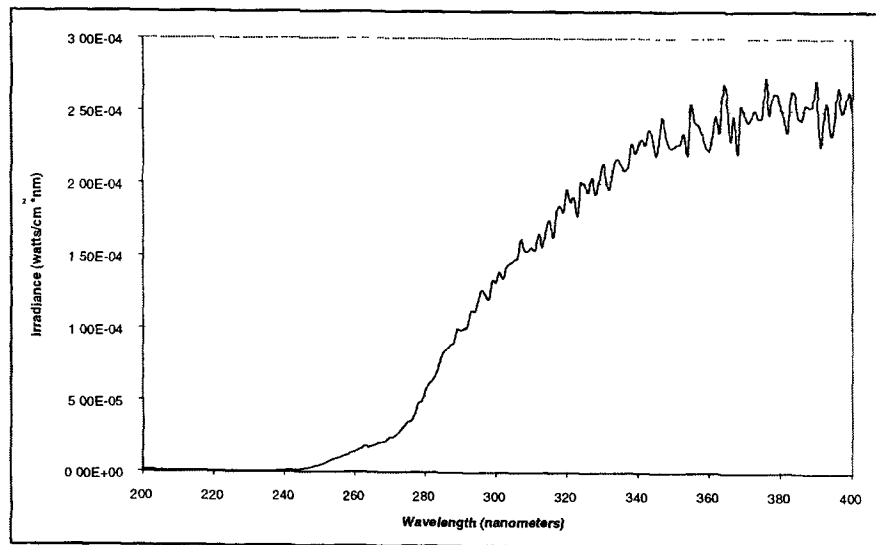


Figure 3. Spectral Output of the Enhanced UV Source

The sample holder, shown in Figure 4, allows two samples to be tested simultaneously and has one solid disk in the top position used as the reference source for the electrostatic probe. This sample holder assembly is movable within the vacuum chamber for fine adjustment of the separation distance between the voltage probe and the sample surface.

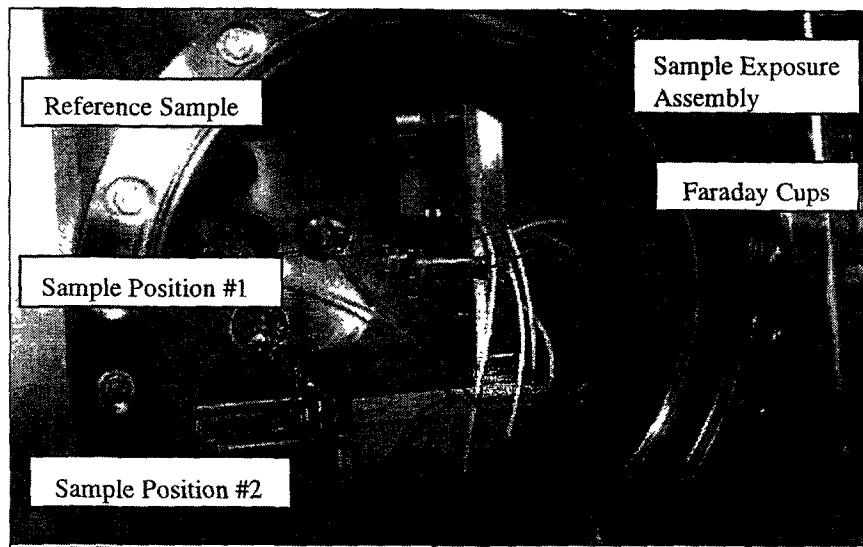


Figure 4. Mobile Sample Holder Assembly

Two Faraday cups, shown in Figure 4, are mounted on the sample holder between the two sample coupons. Each of these Faraday cups have a 0.07cm^2 aperture used to measure the electron beam current density. A digital current integrator monitors one Faraday cup. Digitized output (electron counts) from the current integrator is read by the data acquisition system and used to control events. A second Faraday cup is monitored by a sensitive electrometer for continuous logging of current density data.

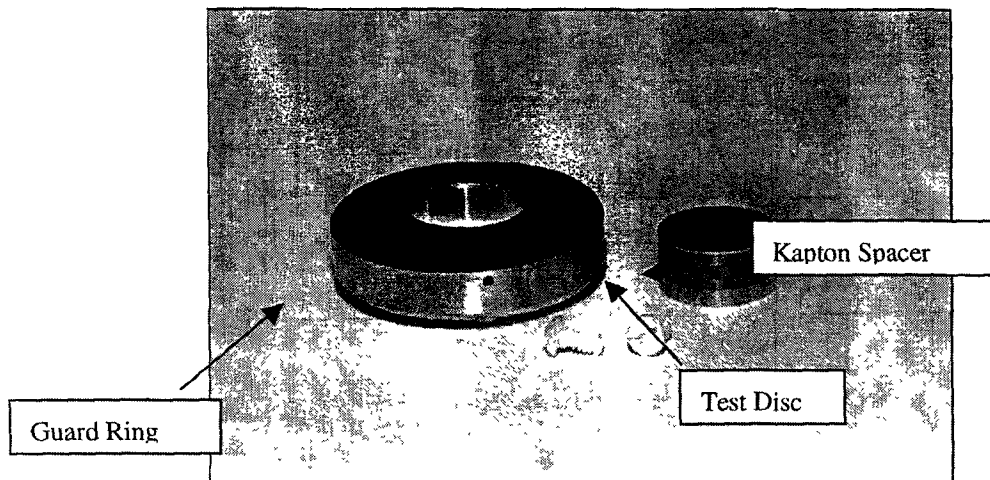


Figure 5. Sample Coupon.

The sample coupon shown in Figure 5 was made of 6061-T6 one-half inch thick aluminum alloy. A schematic side view is provided in Figure 1. Sample coupons consisted of an outer (guard) ring and inner (test) disc. The test disc was secured within the guard by means of a rear mounted

0.06-inch thick Teflon™ disc and mounting screws. The test disc sample area is 2.85cm^2 and is isolated from the guard ring with 1mm thick Kapton™ tape. The total sample area is 15.5cm^2 , an aspect ratio of approximately 5 to 1. Each sample coupon was secured to the sample holder by threading the test disk to an insulated mounting bolt. This was wired via a vacuum electrical feed-through to the current monitoring device. Sample surface to voltage probe separation was adjusted and the guard ring connected to chamber ground.

Surface voltage of the coating is measured by means of an electrostatic probe mounted on a pneumatic linear motion vacuum feed-through. A Trek Model 344 Electrostatic Voltmeter has a measurement range from 0 to 2kVDC with an accuracy $\pm 0.1\%$ of full scale. The voltage probe, attached to a linear motion vacuum feed-through, translates the probe to the required sample position for a surface voltage measurement.

Initially sample coupons were coated across and over the Kapton separator located between the inner and outer sections of the sample coupon (see Figure 5). This was changed when it was found to result in a charge collecting area larger than expected. As a result of these findings, sample coupons were coated before assembly to ensure that the gap between the inner and outer coupon sections was not coated. This change in coupon coating configuration helped to ensure that a charge collecting area was confined to the inner disc of a coated sample coupon.

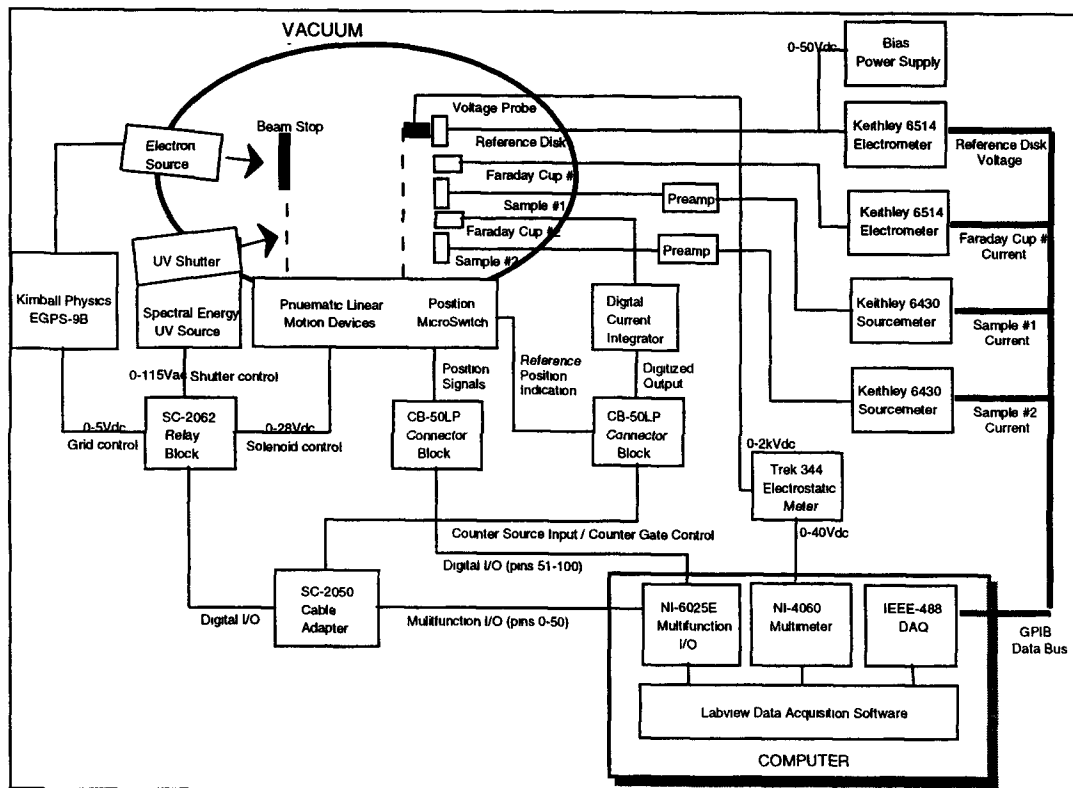


Figure 6. Conductivity Test System Control & Data Acquisition

The data acquisition system layout, shown in Figure 6, is custom designed to implement system controls and perform data storage operations. Utilizing National Instruments hardware and Labview Software this system is programmed to perform:

- Translation of pneumatic linear motion devices for blocking the electron beam and moving the electrostatic probe into position for a surface voltage measurement,
- Shuttering of the ultraviolet light,
- Suppression of the electron beam,
- Communicating with GPIB devices,
- Event timing,
- Data-logging operations,
- System error handling.

During an exposure test, Faraday cups (see Figure 6) mounted near the samples produce a current proportional to that of the electron beam current density. The digital current integrator measures this coulomb charge and produces a digitized output relative to the number of incident electrons per unit area. This digitized output (electron counts) is used to control timing events.

Table 2 provides a listing of the test equipment used to provide the electronic components used to operate and acquire data from this unique space simulation test chamber. Use of dual radiation sources allowed AZ Technology and NASA investigators to evaluate the effects of two typical but very different energy sources naturally occurring in space. Invacuo electrical measurements during space simulation irradiation testing provide insight into possible different degradation mechanisms and how they effect the new generation of semiconductor thermal control coatings.

Table 2. Conductivity Research Equipment

Equipment	Manufacturer / Model	Description
Electron Source	Kimball Physics	Beam Energy: 1keV to 50keV
	Model EFG-9 Electron Flood Gun	Beam Current: 10^{-9} A to 10^{-4} A
UV Source	Spectral Energy	Xenon Lamp
		Dichloric Lense
Electrostatic Voltmeter	Trek Model 344	Voltage measurement range: 0 to • 2kVDC
		Measurement accuracy: • 0.1% of full scale
Current Measuring Devices	Keithley Model 6430	Sub-Femtoamp Remote Sourcemeter: 100aA sensitivity
	Keithley Model 6415	Electrometer: 100aA sensitivity
	EG&G Ortec Model 439	Digital Current Integrator
	EG&G Ortec Model 996	Counter & Timer
Data Acquisition System		Pentium 300Mhz Computer System
	Microsoft	Windows 95
	National Instruments	Labview Software Version 5.0
	National Instruments NI-6025E	PCI multifunction I/O Card
	National Instruments NI-4060	PCI Digital Multimeter
	National Instruments SC-2062	Electromechanical relay board
	National Instruments SC-2050	Cable Adapter Assembly
	National Instruments CB-50LP	Connector Block

Figure 7 provides a general configuration layout of the test chamber. The electron flood gun and the NUV source are each offset by 5.5 degrees in the horizontal (Z) axis from normal and are normal to the samples in the vertical (Y) axis. This minimizes the offset angle to the sample, while providing sufficient separation.

NUV source was equipped with a dichroic infrared (IR) energy filtering system to minimize sample heating. Both sources were located at a sufficient distance from the samples that resulted in coverage of all test samples and detectors with a uniform beam. A UV grade quartz window was used to allow the externally mounted NUV source radiation to pass into the vacuum test chamber. The entire system was pumped down using a vacuum turbo pump. Samples were exchanged through a 10-inch diameter quick access door airlock combines with a viewport.

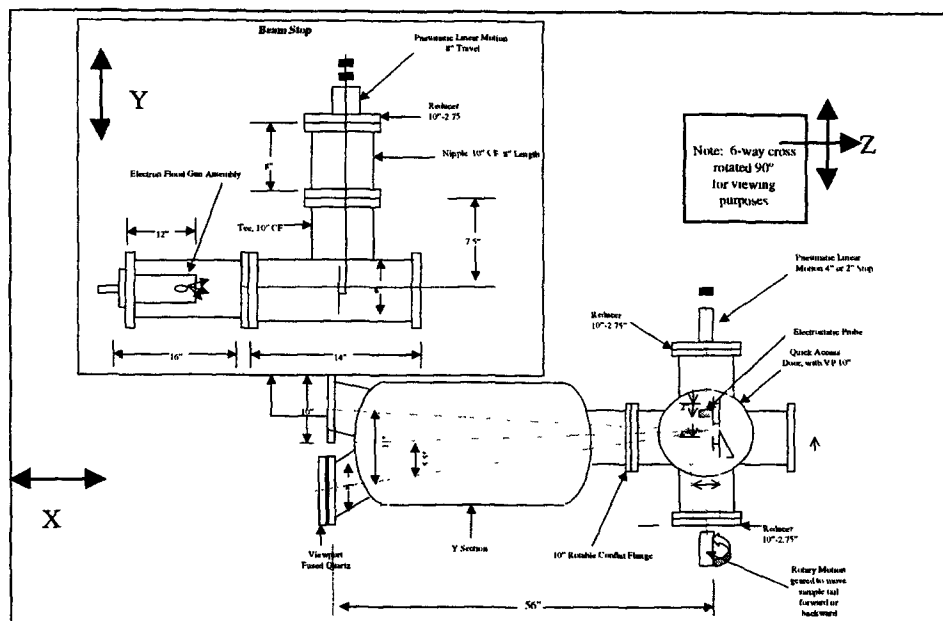


Figure 7. General Layout of Conductivity Test System

2.2.2 Test Procedure

Each sample coating was tested in exactly the same manner. Thermal-optical property evaluation and thickness measurements were performed on each coating sample. Additional samples were produced from the same paint batch for a surface resistivity measurement to be made with the Hewlett Packard high resistance test meter and resistivity cell. This measurement was performed at atmospheric pressure under an argon purge. Results from these tests are shown in Table 3.

Table 3. Pre-Exposure Test Measurements

Sample	Batch	Emittance	Alpha	Thickness (mils)	Thickness (cm)
AZ-70	I-041	0.892	0.122	9.3	0.023622
AZ-93	H-209	0.913	0.155	5.1	0.012954
AZ-100	I-039	0.911	0.150	5.4	0.013716
AZ-400	I-040	0.902	0.295	3.4	0.008636
AZ-1000	H-215		0.963	2.9	0.007366
AZ-2000	H-212	0.916	0.238	3.21	0.0081534
AZ-2100	I-043	0.893	0.153	6.91	0.0175514
TMS-800	I-048	0.876	0.352	3.82	0.0097028
TMJ-810	I-044	0.890	0.242	3.79	0.0096266
AZX-S1	I-055	0.852	0.144	5.09	0.0129286
AZX-SG1	I-053	0.892	0.352	3.61	0.0091694
AZX-SG2	I-054	0.895	0.376	3.75	0.009525

Solar absorptance and thermal emittance of test samples were measured at AZ Technology and received at MSFC/ED31 using the Laboratory Portable Spectroreflectometer (LPSR) instrument and the Temp 2000 emissometer. Each sample had a 1mm Kapton™ tape placed in the spacing between the guard ring and the test disc and then was assembled. The samples were then positioned as either as “Sample 1” or “Sample 2” on the movable sample holder within the vacuum chamber. A vacuum environment of less than 1×10^{-6} Torr is required for testing. Exposures began only after a one-hour warm-up of the electron source, UV source, and electrostatic meter. Each sample exposure follows the procedure described in Table 4.

Table 4. Sample Exposure Procedure

Run	Exposure Description	Current Setting	Counts	Discharge Data
1	10keV electrons	1na/cm ²	2500	Sample #1
2	10keV electrons	1na/cm ²	2500	Sample #2
3	10keV electrons	5na/cm ²	2500	Sample #1
4	10keV electrons	5na/cm ²	2500	Sample #2
5	10keV electrons	10na/cm ²	5000	Sample #1
6	10keV electrons	10na/cm ²	5000	Sample #2
7	10keV electrons + UV	1na/cm ²	2500	Sample #1
8	10keV electrons + UV	1na/cm ²	2500	Sample #2
9	10keV electrons + UV	5na/cm ²	2500	Sample #1
10	10keV electrons + UV	5na/cm ²	2500	Sample #2
11	10keV electrons + UV	10na/cm ²	5000	Sample #1
12	10keV electrons + UV	10na/cm ²	5000	Sample #2

A snapshot method was used to take measurements of the sample coating's surface voltage and current flowing through the coating. Snapshot measurement was obtained during an exposure run and the sequence begins only when the data acquisition system has logged the required interval of electron counts. Snapshots occur approximately every 100 electron counts with the following sequence:

- 1) The voltage probe is in the reference position, as shown in Figure 8. A measurement is made of the reference disk that has been biased to a known voltage potential. This measurement is then compared to the known bias voltage and the resulting offset used as a correction factor for the upcoming surface voltage measurements.

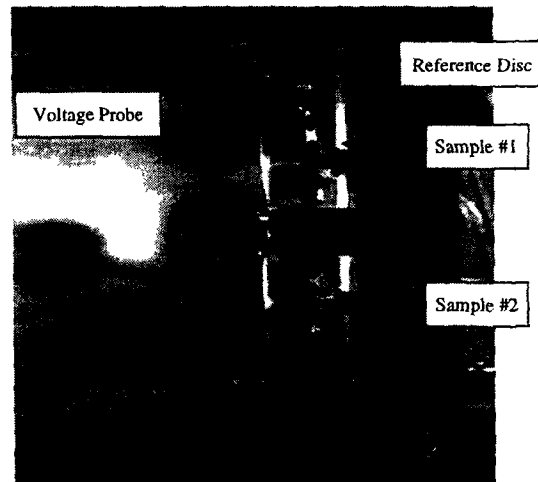


Figure 8. Probe in Reference Position

- 2) The current passing through sample #1 is logged to file.
- 3) Probe is remotely controlled to move to sample position #1, as shown in Figure 9. A surface voltage measurement of sample #1 is made and logged to file.

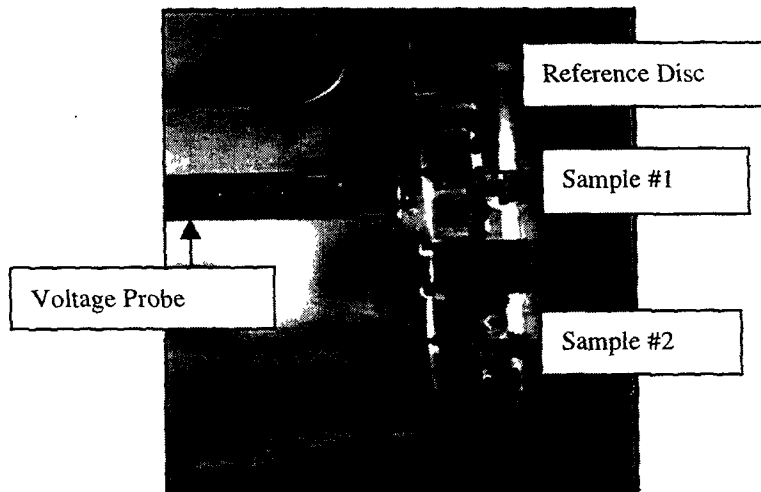


Figure 9. Probe in Sample #1 Position

- 1) The current passing through sample #2 is logged to file.
- 2) Probe is remotely controlled to move to sample position #2, as shown in Figure 10. A surface voltage measurement of sample #2 is made and logged to file.

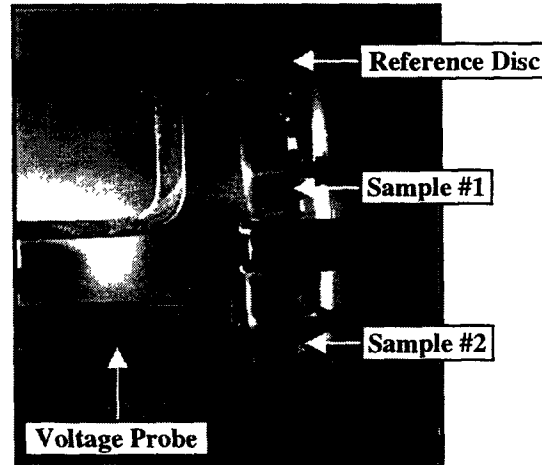


Figure 10. Probe in Sample #2 Position

- 3) The probe is remotely controlled to move back to reference position, where it remains until the next snapshot sequence is triggered.

Exposure runs one through six were electron beam exposures only. Exposures seven through twelve were combined UV and electron exposures. For each exposure run:

- 4) The electron beam current density was stored to file and integrated into electron counts that controlled exposure events,
- 5) The current through the sample coatings were continuously measured (ten samples/second) and stored to file,
- 6) Surface voltage measurements (snapshots) were periodically made for each sample.

Exposure runs are made concurrently with the elapsed time between exposures varying from 1 to 30 minutes. Each sample received an exposure of 40000 electron counts and 6.25 equivalent sun hours (ESH). One electron count is equal to 1×10^{-10} coulombs or 7.9×10^9 electrons/cm². Each sample received a total fluence of 3.16×10^{14} electrons/cm².

3.0 TEST RESULTS

The following is a description of each coating that was tested:

AZ-70	Inorganic white, nonspecular thermal control coating
AZ-93	Inorganic white, nonspecular thermal control coating
AZ-100	Developmental inorganic white, electrically dissipative thermal control coating
RM-400	Epoxy white, electrically conductive thermal control coating
AZ-1000	Inorganic semi-conductive black thermal control coating
AZ-2000	Inorganic semi-conductive white thermal control coating
AZ-2100	Developmental inorganic white, electrically dissipative thermal control coating
AZX-S1	Developmental inorganic white, electrically dissipative thermal control coating
AZX-SG1	Developmental inorganic white, electrically dissipative thermal control coating
AZX-SG2	Developmental inorganic white, electrically dissipative thermal control coating
TMJ-810	Inorganic yellow nonspecular semi-conductive marker coating
TMS-800	Inorganic yellow nonspecular marker coating

Table 5. Solar Absorptance Values for Pre and Post Irradiated Test Samples

Sample	Batch	Pre-Alpha	Post-Alpha	Percent Change
AZ-70	I-041	0.122	0.123	-0.82%
AZ-93	H-209	0.155	0.162	-4.52%
AZ-100	I-039	0.150	0.149	0.67%
RM-400	H-213	0.295	0.329	-11.53%
AZ-1000	H-215	0.963	0.967	-0.42%
AZ-2000	H-212	0.238	0.250	-5.04%
AZ-2100	I-043	0.153	0.148	3.27%
TMS-800	I-048	0.352	0.359	-1.99%
TMJ-810	I-044	0.242	0.249	-2.89%
AZX-S1	I-055	0.144	0.145	-0.69%
AZX-SG1	I-053	0.352	0.365	-3.69%
AZX-SG2	I-054	0.376	0.377	-0.27%

3.1 Spectral Solar Absorptance

Solar absorptance measurements were obtained using the LPSR-200 laboratory portable spectrophotometer instrument both before and after the sample exposure procedure (see Table 4). The resulting solar absorptance (alpha) for each coating is shown above in Table 5. Spectral solar absorptance curves data for each of the coatings are separately plotted in Appendix 'A'. Solar absorptance measurements were performed after the chamber was purged with nitrogen. This significantly reduces the rate of bleaching of the test samples. Experiments done by James Zwiener and David Edwards at MSFC have shown that purging of the space simulation chamber with nitrogen gas for repress, reduces sample bleaching. In addition, Michel Michishnek, of the Aerospace Corporation, has demonstrated the same effect in his space simulation test chambers. Bleaching of a test sample is the reduction or elimination of optical changes (usually

damage) caused by exposure to one or more radiation sources during a simulated or actual space environment test. As a result, the nitrogen purging technique was used for this program to significantly reduce the rate at which a test samples bleach since the chamber was not configured for insitu optical measurements. These optical changes typically occur in seconds or fractions of seconds with most materials but can continue for months or years as shown by Don Wilkes and James Zwiener in the Optical Properties Monitor (OPM) science report to NASA. The OPM materials flight experiment performed solar absorptance measurements as well as other types of optical measurements on materials while on orbit. OPM transmitted stored data back to earth typically on a weekly basis.

3.2 Surface Voltage

Periodically, through each exposure run, a snapshot of each sample surface voltage was made. The custom designed data acquisition (Labview Version 5.1) software controlled the snapshot event sequence. Every one hundred electron counts, the electrostatic probe was positioned above the center of the sample coupon to measure the surface voltage. These surface voltage measurements were stored to a file, designated for a given exposure run and sample. Measurements were logged and referenced to the accumulated number of electron counts.

A total of twelve exposure runs were performed. The first six exposures were performed with only the electron beam operating, while the following six exposures were with the combined electron beam and ultraviolet light. The effect of changing electron beam current density was investigated at three energy levels. Each had two exposures at 1nA/cm^2 , 5 nA/cm^2 and at 10nA/cm^2 current densities. For each exposure run, the median (the median is the number in the middle of the set of numbers, half the data set numbers have values greater than the median and half of the numbers have values that are less) data point was determined for surface voltage for each sample. As a representative surface voltage or "exposure" current density, the two median values of the repeated current density exposures were averaged. This average surface voltage potential versus the exposure sequence, is listed in Table 6. Materials are listed by the magnitude of surface voltage.

The measured surface voltage data from the electron beam exposures are plotted in Figure 11. The surface voltage data from these combined (electrons and UV) exposures are plotted in Figure 12. A comparison of the surface voltage measured during the electron beam exposures and the combined exposures are charted in Appendix B.

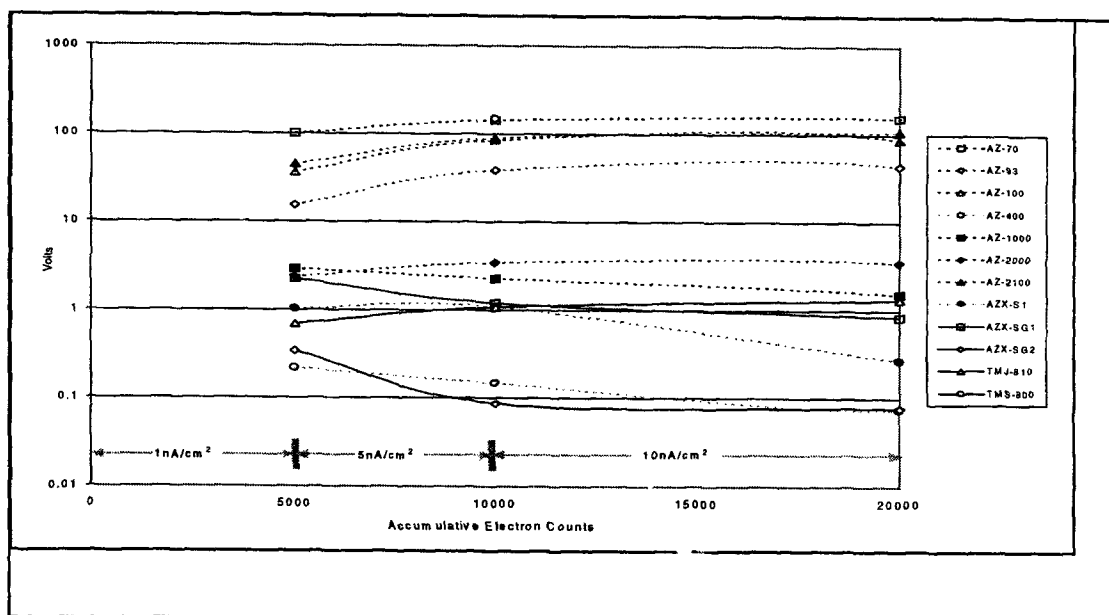


Figure 11. Coating Surface Volts measured during electron beam exposure

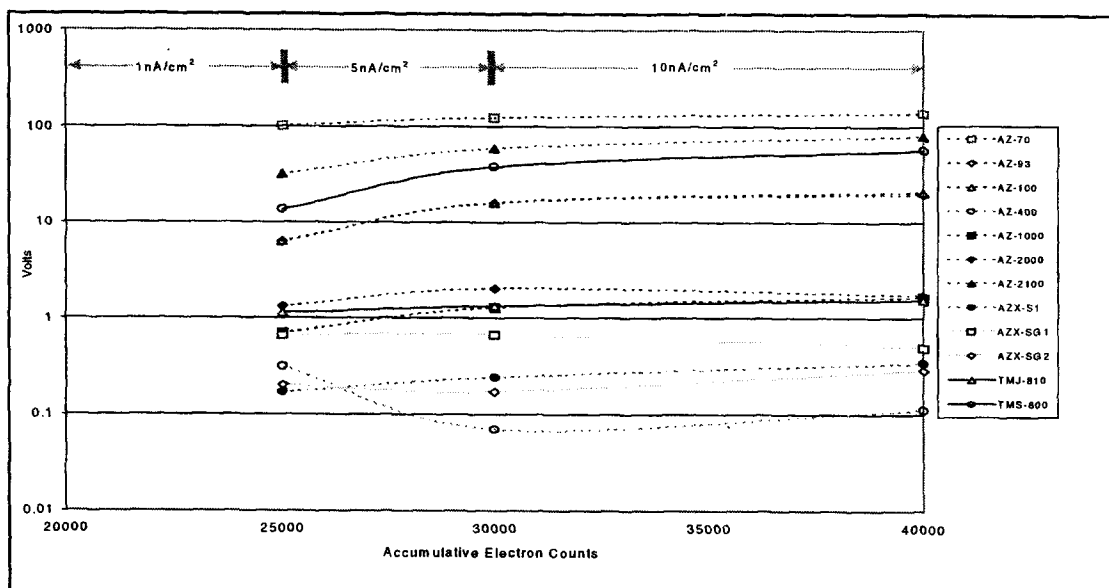


Figure 12. Coating Surface Volts Measured During Combined Electron Beam and Solar UV Exposure

The accuracy of the electrostatic voltmeter is 0.1% of full scale with a measurement range of ± 0 to 2kVdc. Therefore, data files have been grouped into those that measured greater than two volts and those that measured less than two volts. These surface voltage charts are shown in Figures 13 and 14.

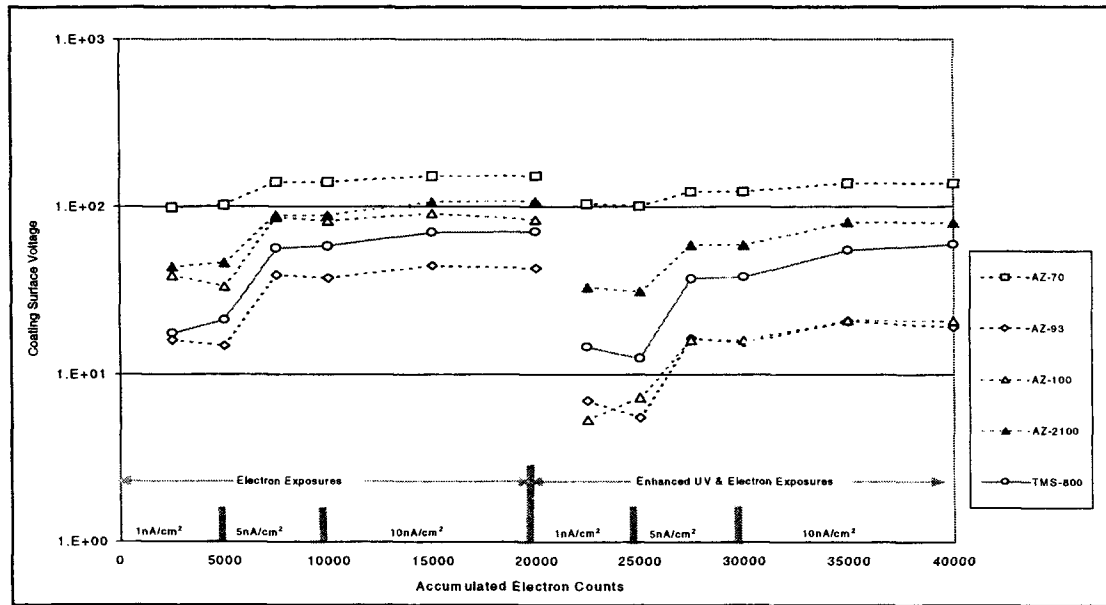


Figure 13. Surface Voltage (greater than 2 volts) Versus Exposure Dose

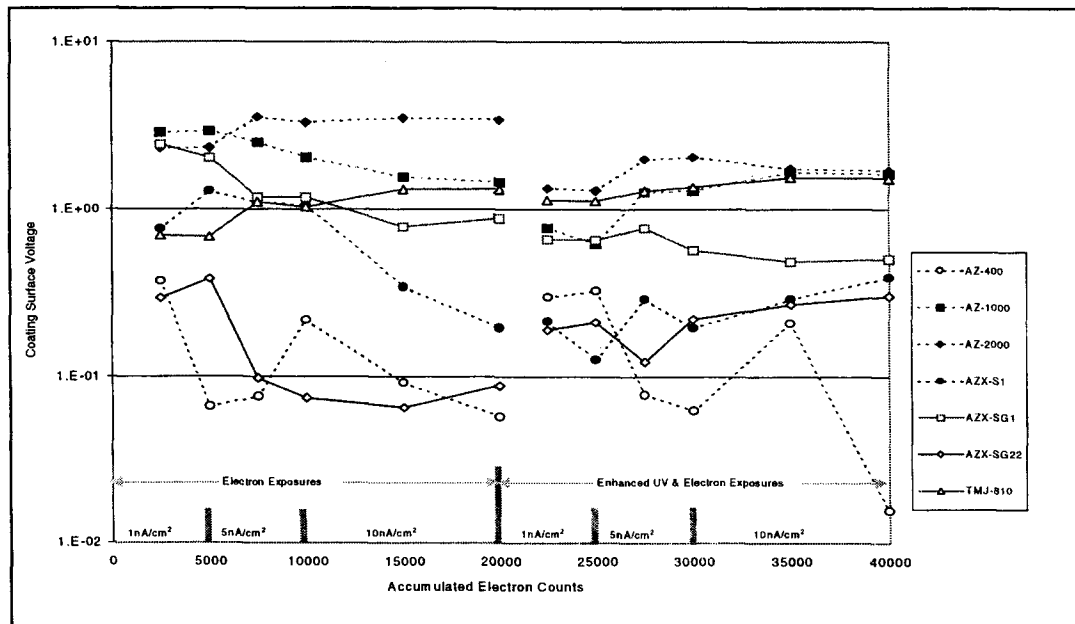


Figure 14. Surface Voltage (less than 2 volts) Versus Exposure Dose

3.3 Conductivity

The conductivity values computed from data measured during the electron beam exposures are plotted in Figure 15. During the combined (electrons and UV) effects exposures, a phenomenon occurs that reduces the measured surface voltage, thereby increasing the possibility of error in the calculation of conductivity. The phenomenon may be caused by changes in the coating, photoelectron emission, or other causes not yet determined. These conductivity values computed during the combined effects exposures are plotted in Figure 16.

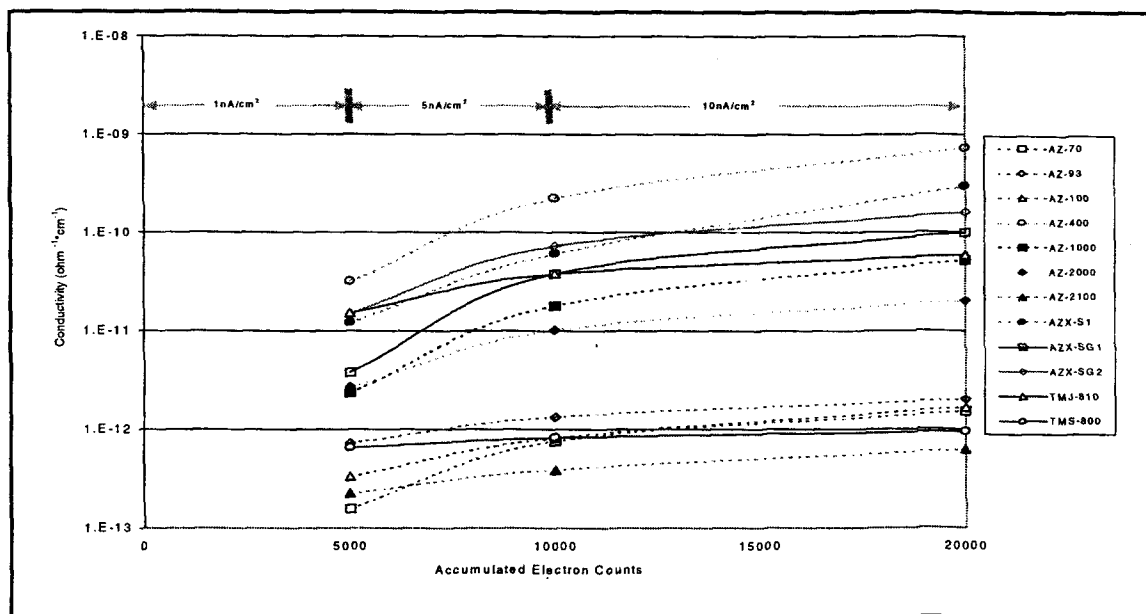


Figure 15. Conductivity Values Derived from Electron Beam Exposure Data

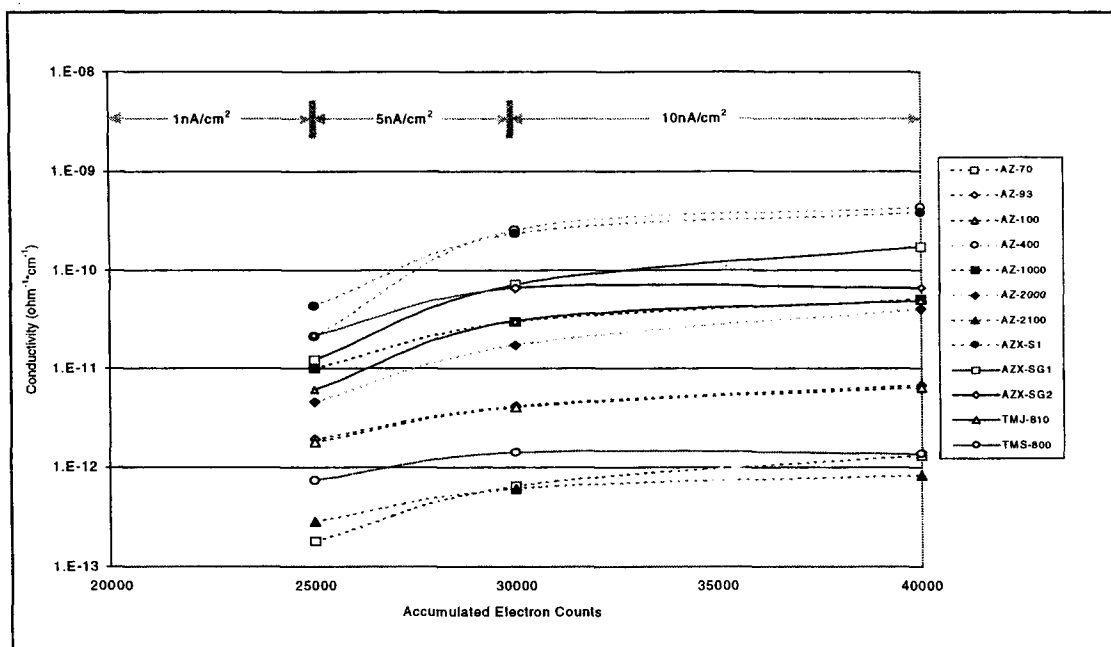


Figure 16. Conductivity Values Derived from Combined Electron Beam and Ultraviolet Light Exposure Data

The accuracy of the electrostatic voltmeter was 0.1% of full scale with a measurement range from 0 to ± 2 kVdc. Therefore, coatings with measured voltage potentials greater two volts are plotted separately in Figure 17. Coatings that measured voltage potentials less than or equal to two volts are plotted in Figure 18. These coatings displayed conductivities in excess of the measurement range of the voltage probe and are shown for reference only.

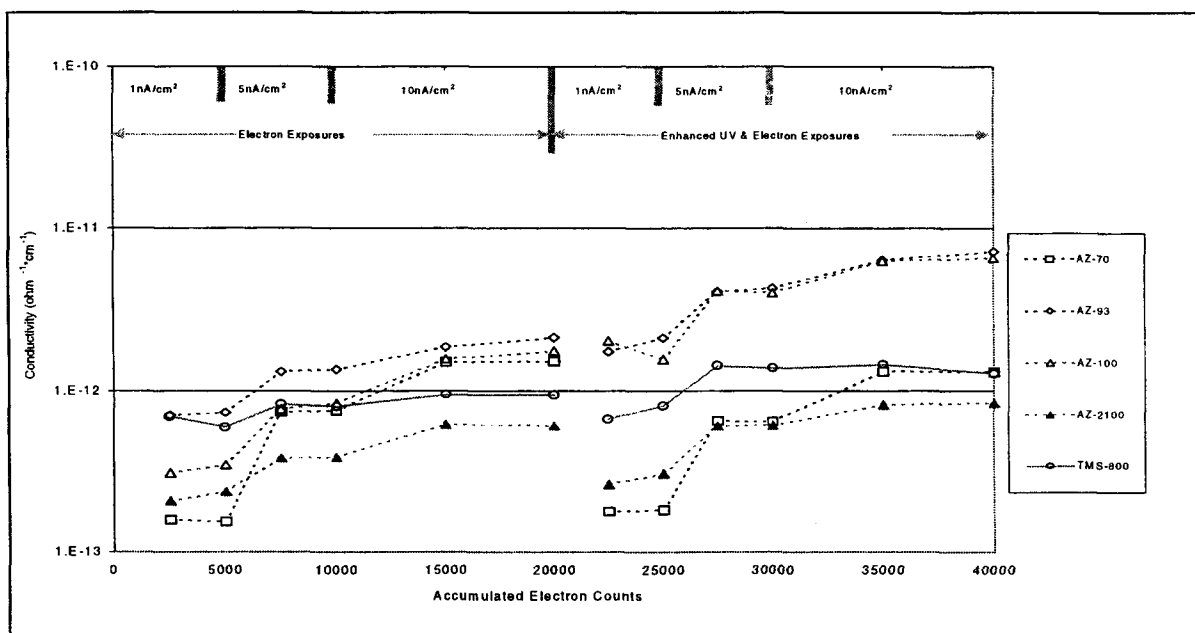


Figure 17. Conductivity versus Exposure Dose (surface voltage greater than 2 volts)

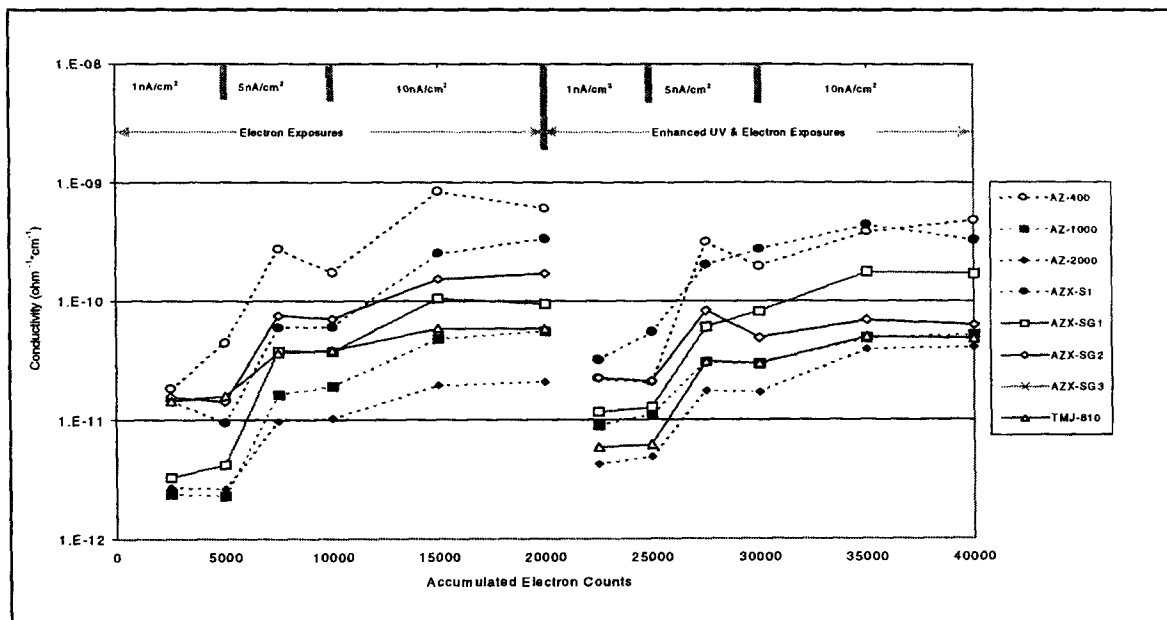




Figure 18. Conductivity versus Exposure Dose (surface voltage less than 2 volts)

A comparison of the computed conductivity values measured during the electron beam exposures and the combined electron beam and solar UV exposures are charted in shown in Appendix B.

Table 6. Surface Voltage Measurements

Material Coating	Surface Voltage					
AZ-70	-101	-141	-153	-102	-123	-138
AZ-2100	-46	-89	-108	-32	-59	-81
TMS-800	-19	-57	-70	-14	-38	-59
AZ-100	-35.8	-82.8	-84.7	-6.2	-16.1	-20.4
AZ-93	-15.4	-37.8	-44	-6	-15.7	-20
AZ-2000	-2.3	-3.4	-3.5	-1.3	-2	-1.7
AZ-1000	-2.9	-2.1	-1.6	-0.7	-1.3	-1.6
TMJ-810	-0.3	1	1.2	1.1	1.4	1.5
AZX-SG1	-2.2	-1.2	-0.8	-0.65	-0.66	-0.5
AZX-S1	-1	-1	-0.27	-0.17	0.24	0.34
AZX-SG2	-0.38	-0.1	0.08	0.2	0.22	0.3
RM-400	-0.2	-0.2	-0.1	0.2	0.15	0.2

Electron Exposure Current Density (nA/cm ²)					
					
5000	10000	20000	25000	30000	40000

Increasing UV Exposure (equivalent sun hours)		
		
4.5	5.5	6.5

4.0 ELECTRICALLY CONDUCTIVE CERAMIC PIGMENTS

AZ Technology has identified and done initial evaluation on a number of new inorganic pigments. These materials have lower solar absorptance values than those identified in previous research. These compounds had metal atoms that were specifically chosen because of their known or theoretical potential to produce low absorptance metal oxides in the UV through the NIR from previous research. Therefore, AZ Technology took the approach of producing oxides and/or alloying known high reflectance substances to other metals (starting as organo-metals) or metal oxides. In so doing, AZ Technology could potentially solve or decrease the impact of several problem areas that reduce the usefulness of thermal control coatings. The first is decreasing the solar absorptance of the TC coating to be more efficient in rejecting solar energy. Second is stabilizing the chemical structure against ion or free radical formation from solar radiation, hence decreasing degradation of these materials. Third is providing surface charge buildup protection through the formation of a semi-conductive pigment or additive.

Table 7. Current Candidate Metal Atoms and Their Use in This Program

Metal Atom	Chemical Designation	Application
Rhenium	Re	
Rodium	Rh	
Ruthenium	Ru	
Rubidium	Rb	

4.1 Evaluation of Coating Additives and Binders

AZ Technology continues to acquire new coating materials where possible, such as potential binder additives potassium hexafluorosilicate and potassium perchlorate. Each one of these compounds can be used to aid in the stabilization of a thermal control coating. Potassium hexafluorosilicate could be used as a means to impede the loss of oxygen from the primary pigment. This is hypothesized to being possible because of the dense tightly bound electron cloud structure that resided around this compound. We intend to investigate the possibility that the use of such a compound will tend to inhibit the depletion of oxygen from the pigment that is used in a thermal control (TC) coating. Because of the dense electron cloud of this compound, it may help or at least impede an ionized oxygen atom from diffusing out of the coating matrix by electron donation or simple charge repulsion.

Another approach is the use of a perchlorate compound, specifically potassium perchlorate and ammonium perchlorate. The purpose of using this type of compound as an additive in a thermal control coating, is to act as a supplemental source of oxygen, since the for most white TC coatings degrade through the loss of oxygen. Presently, there has been no success introducing this material directly into a silicate binder. When the perchlorate came into contact with the silicate solution, precipitation of the silicate occurs and forms a solid. The precipitated silicate is rendered useless as a binder in this state.

A few other alternatives still can be evaluated. One is to purposely mix the perchlorate with silicate while mixing at high speed, thus potentially producing a homogenous solid that then could be ground and added to a coating. Second is to blend the perchlorate with the pigment and determine if the pigment will act as a buffer slowing down or stopping the rapid solidification that now occurs.

A new type of binder material was also evaluated. It is currently a Boeing proprietary material that is supplied to AZ Technology to determine it's utility for space applications. The reason for doing some evaluation of it for this program is its transparency, Figure 19 vs. that of a potassium silicate as shown in Figure 20. This new material has promise, because of the fact that not only does it have very good transmittance, more importantly, it under goes significant shrinkage during the curing process. The shrinkage characteristic of this binder material is very important because of several aspects.

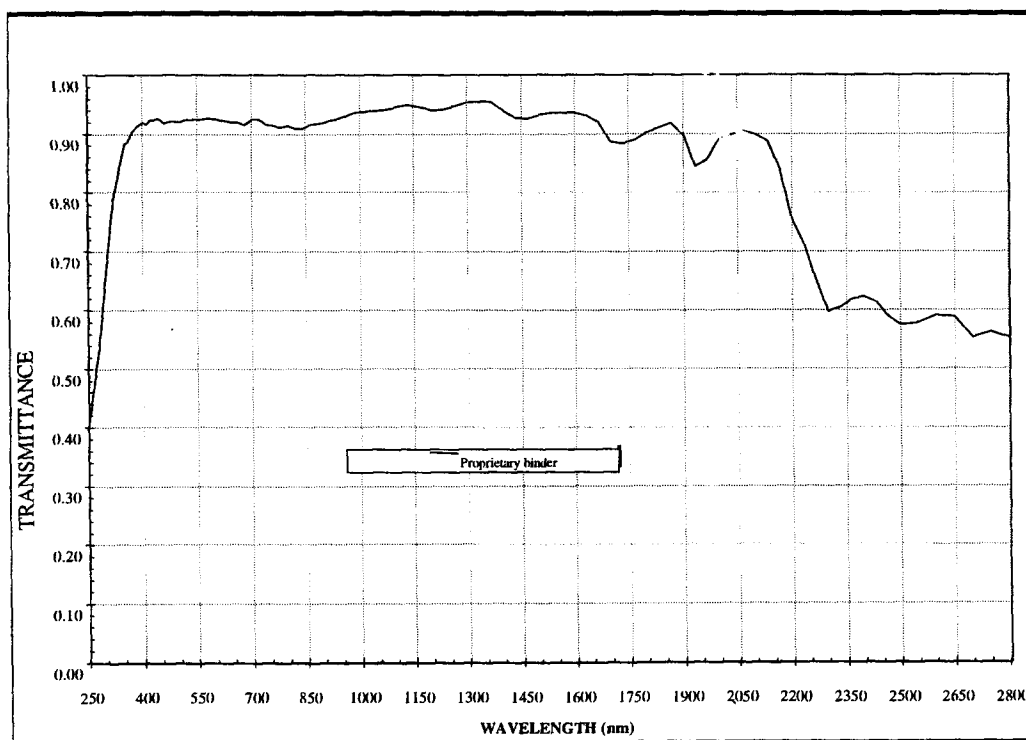


Figure 19. Transmittance of Boeing Binder Through the Solar Spectrum

First, in this limited study, the binder does not degrade mechanical bonding to an aluminum substrate as a consequence of shrinking. Two, this binder does not seem to lose physical adhesion, nor does it appear to crack or fracture during this process, even as a neat film compound. Third, a binder that shrinks as part of an electrically conductive coating curing process without fracturing, forces the conductive particles to be pulled together. Binder shrinkage without crack propagation should result in a more efficient conductive coating. Hence, AZ Technology hopes that the hypothesis relates to the physical and mechanical performance of this new binder is proven to be accurate.

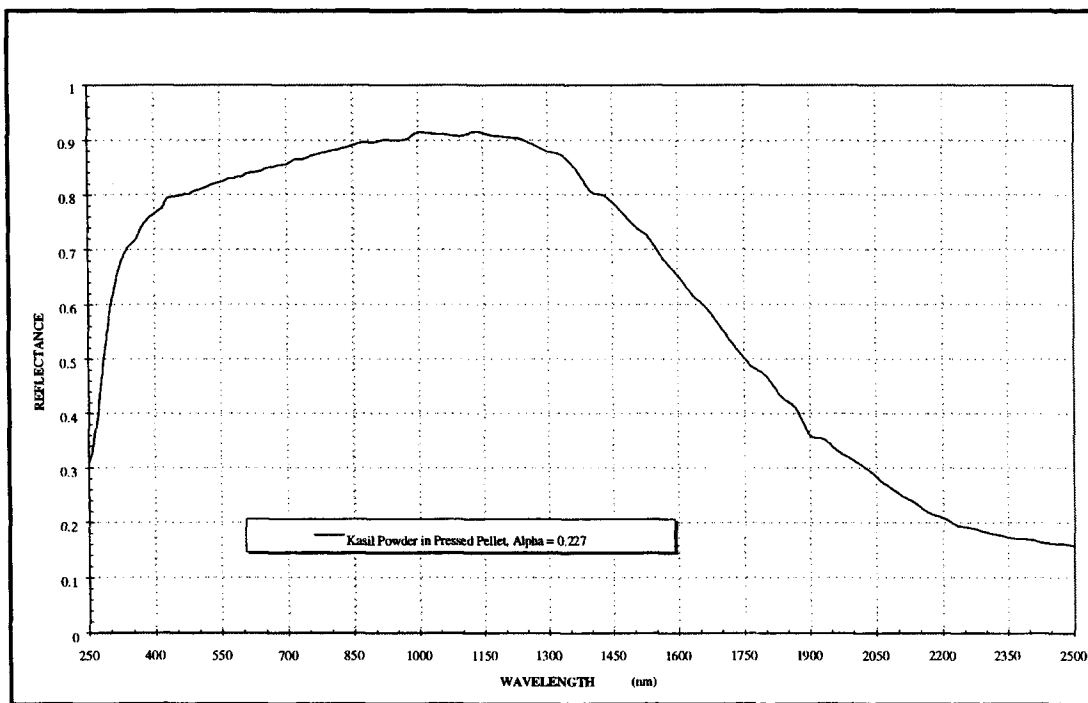


Figure 20. Solar Absorptance of Potassium Silicate Binder

To demonstrate the potential of this binder AZ Technology currently has produced a coating using this potential binder and calcined zinc oxide, shown in Figure 21. With a pigment loading less than that used for AZ-93 and a similar cured coating thickness of 4.5 mils, we achieved a comparable solar absorptance value of about 0.155. For a first attempt, these results were quite promising.

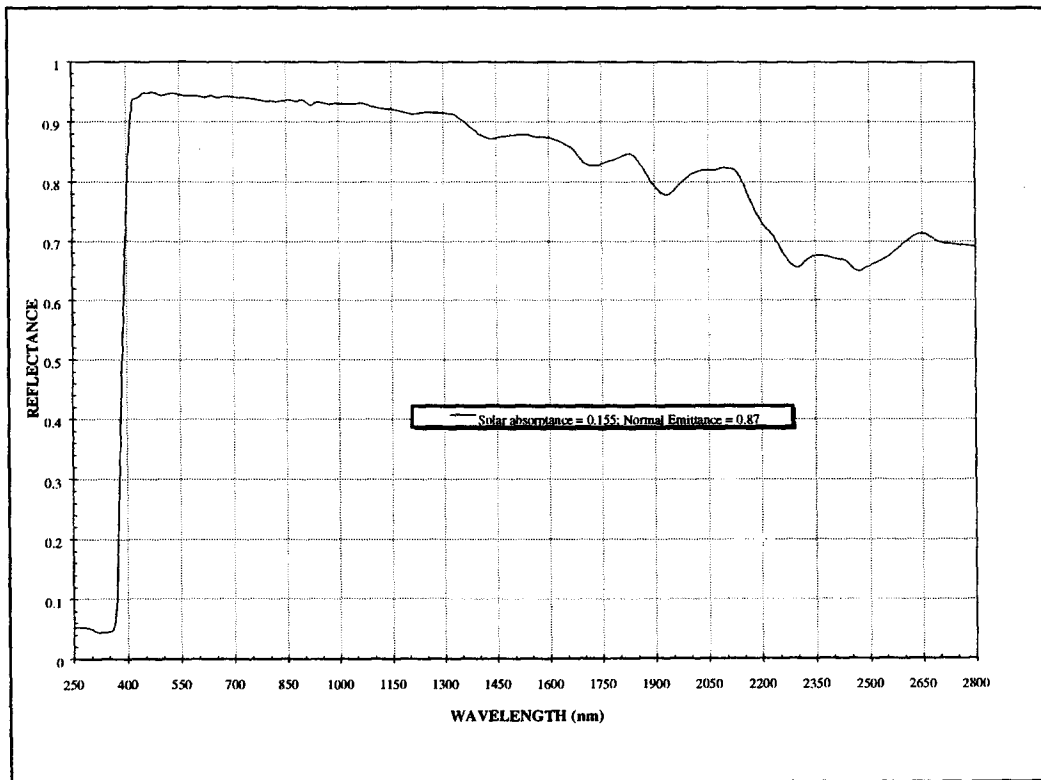


Figure 21. Solar Absorbance Zinc Oxide Pigmented Proprietary Binder

4.2 Optimization of Electrically Conductive Ceramic Pigments

During this program, AZ Technology was engaged in the development of whisker type material that had good conductivity. Some initial development on such material was conducted under the SBIR program, but little progress could be made because of our focus on basic semiconductors that could be produced having a color of white or black.

The synthesis and production of a whisker like semiconductor material will provide a much better mean free electrical pathway for electrons to flow than the relatively poor one produced by the typical particle to particle contact. AZ Technology did discover in a previous study that very white and electrically conductive whiskers could be produced. But the yield was very low and the whiskers were almost impossible to separate and collect from the nonconductive residue left behind after the reaction was finished.

The approach taken in this program is to use what we refer to as supports. The term supports as we use it, means that the semiconductor precursors are deposited on to a whisker (short fiber). The supports that we are using are commercially available by products of the composite industry and are available in a variety of materials. The types of materials available, range from carbon to zirconium oxide. Processing starts by producing a solution that will react to form the semiconductor. In AZ Technology's current process, the solution of semiconductor precursors overcoat the supporting whisker with the material. The overcoated support material is then dried and heat-treated to produce the final semiconductor having acceptable optical properties e.g. white, black or transparent.

Although this processing appears easy, and has been successful so far, there still is a need to investigate the various coating parameters and detailed techniques need to be worked out, it is hoped that it will. However, at the present time, the knowledge base in this process is limited. AZ Technology is currently working with four support materials given in Table 8.

Table 8. Support Materials

Material	Rational for use	Color	Dimensions (length by diameter)
Carbon / Graphite	O ₂ Reactive leaves hollow core, and is low mass impact on coating	gray	3-8 mm x 8-12 μ .
Quartz/ Silica	Transparent if mixed with many binders, little effect on solar absorptance	Clear to white	10-14 mm x 20-30 μ
Zirconium oxide	Good reflectance throughout solar spectrum. May help to enhance α_s of some coatings	white	1 mm or less x 8-12 μ .
Silicon carbide	Good support material for black coatings, good documentation in ceramic applications	Gray to black	3-8 mm x 8-12 μ .

The primary challenges are to determine which technique is going to be better to use with supports, and to determine coating material by mass or volume percent. Because we are dealing with whisker materials that have a wide range of densities, determining a good ratio of whiskers to solution is very difficult since we have a wide range of parameters to satisfy. Some of these parameters are solution concentration, viscosity, coating technique, and drying. Even with all of these variables to consider, this seems to be a viable approach as the results of a trial run shows in Figure 22.

As is seen in Figure 22, using the previously discussed whisker coating method, formation of the desired type of material can be achieved. These whickers were produced using a carbon support and a fine particle dispersion of tin oxide. The resultant product after heat treating is a white whisker that should provide a good electrical pathway with little effect on the optical properties of the thermal control coatings. The measured resistance was 10^3 to $10^4 \Omega/\square$ in air using only a multimeter and straight probes. It is not likely that we will be able to obtain a more accurate resistance value using the Hewlett-Packard electrical resistance cell, because of the volume of material required, until these whiskers can be incorporated into a coating.

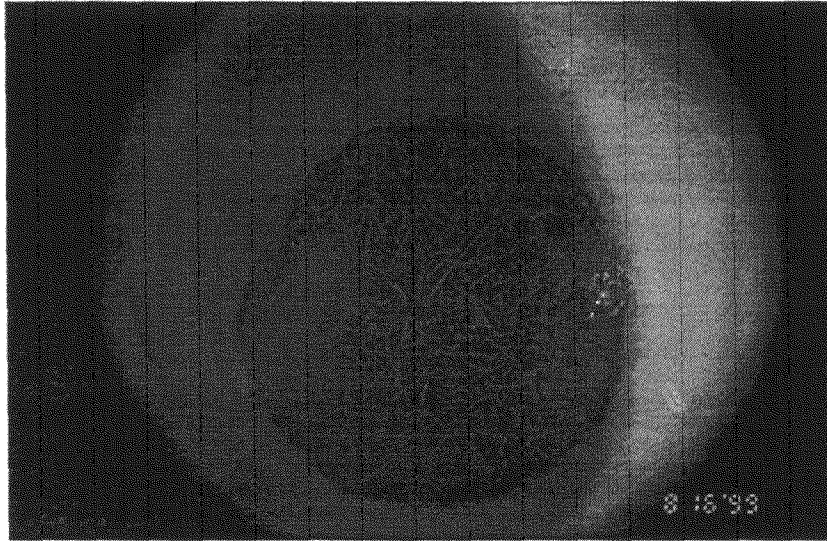


Figure 22. Synthesized Electrically Conductive Whiskers

5.0 CONCLUSION

To judge the performance of the test chamber system, it was decided early in this program to use known coatings that ranged from dielectric to a good semiconductor as reference materials. The AZ-70 was the dielectric, AZ-93 was considered the poor semiconductor and RM-400 a good semiconductor. Preliminary data recorded during the checkout of the test chamber was found to be order(s) of magnitude or decades greater in surface charge than those presented in Table 6 of this report. Early data did follow an expected logical trend, that being, as one tests coatings from dielectric to a good semiconductor the surface charging of the coatings decreases. The AZ-70 (dielectric) coating accumulated a surface charge (electron exposure only at 1na) in the order of approximately 2500 to 2700 volts, AZ-93 (a natural, but poor semiconductor when used in this configuration) accumulated a surface charge in the order of approximately 175 to 225 volts and RM-400 would not accumulate a surface charge during the initial testing. In later tests these same coatings as shown in Table 6 have surface charges of -101 to -153, -15.4 to -44 and -0.2 to -0.1 respectively. This dramatic difference in surface voltage values demonstrates the importance of chamber and test design. It provides scientists and engineers with material data tested using the best up to date system and test methodology known at the time.

Even more import is how materials should be classified for use. Depending on the way materials are classified whether by charge voltage, resistivity or conductivity could have an impact on the cost and time in constructing a spacecraft. If resistivity is used, a much more expensive material may be chosen with a long lead time, instead of a different, readily available material that meet the charging criteria but not the resistivity requirements.

The phenomenon of a reduction in surface voltage upon exposure to UV radiation after being exposed to only electron charged particles is poorly understood. In addition, it is believed that this is the first time that it has been demonstrated using spacecraft thermal control coatings as test samples. Although the magnitude of surface charge reduction is likely to be material dependent, the effect of introduction and removal of UV radiation from an exposed surface is an important factor to be considered by designers and could be used as an advantage for future missions.

Evaluation of the spectra provided in Appendix A, exhibit very little change in the solar absorptance of the coatings tested in this program. If the method and technique for purging the chamber with nitrogen were successful, it demonstrates that all of these coatings have potentially good resistance to the space environment. The RM-400, which had an epoxy binder, was an exception to this and was only used because there was historical data from TSS. It was also known to have and retain good electrical properties over several years.

The experimental coatings tested are all organo-metallic polymers based on nano-technology to produce them. In addition, they have very good conductivity and seem to have potentially very good optical stability. Such experimental coatings may be the way of the future if test chambers like the one are designed and built with other radiation sources and in vacuum solar absorptance measurement capability. In the case with optical measurements, this would eliminate any possible unknowns concerning bleaching of the test samples. With an in-vacuum solar absorptance measurement capability, investigators could also potentially correlate the formation of mobile electron and any change in the materials solar absorptance. It is this investigators theory, that if a coating cannot efficiently conduct away electrons, absorption bands will occur in the near UV, near infrared and the mid-infrared. This will cause an increase in the spacecraft's solar absorptance and potential heating up of the craft. In addition, if the electron charge continues to build up, electrical arcing will occur and damage to or failure of the entire system may result.

Much further work needs to be done using the type of test chamber developed during this program. It could provide invaluable data for many types of materials used on or in a spacecraft. Although there was little opportunity to optimize the coatings tested, this program has provided insight as to how to proceed. The experimental coatings tested during this program will be aided by the data obtained. With further work and understanding, it may be possible to record how current and new materials charge and discharge and eliminate such problems from occurring.

APPENDIX A

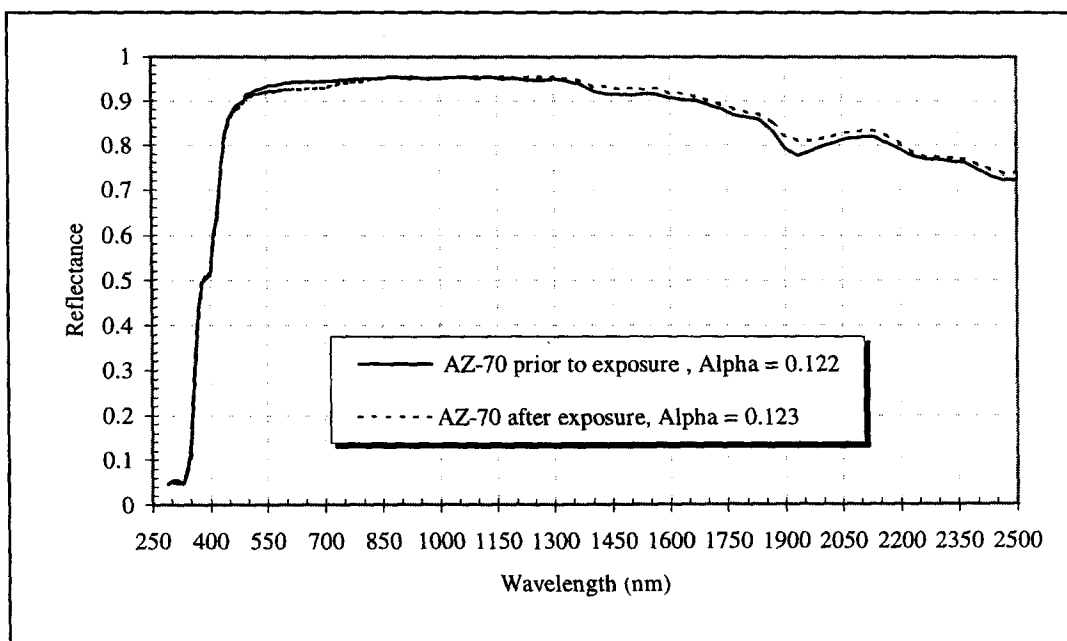


Figure 23. Solar Absorptance of AZ-70

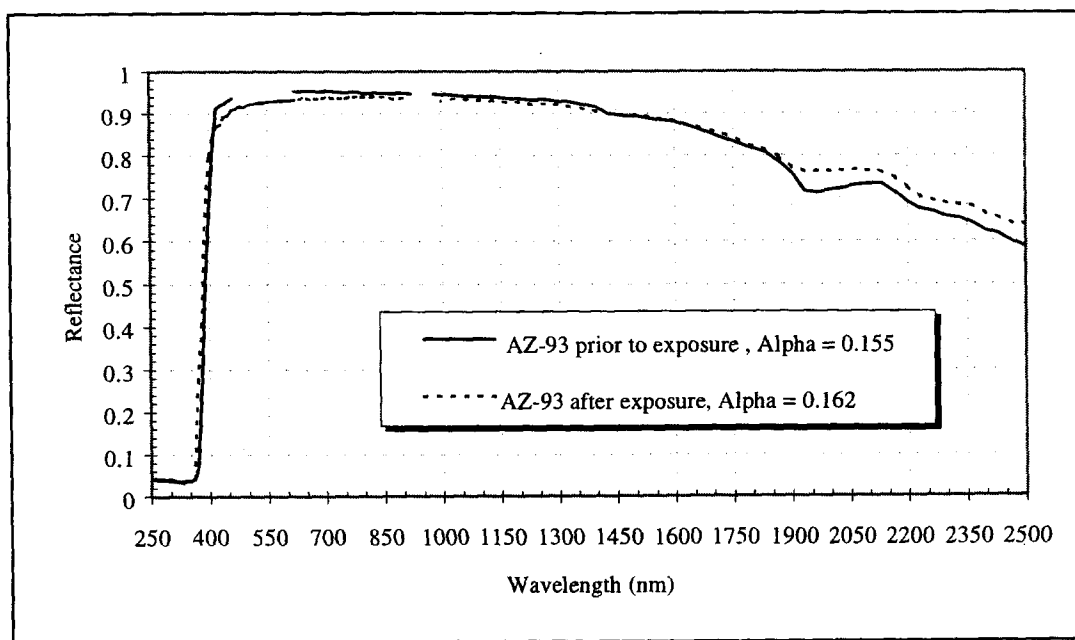


Figure 24. Solar Absorptance of AZ-93

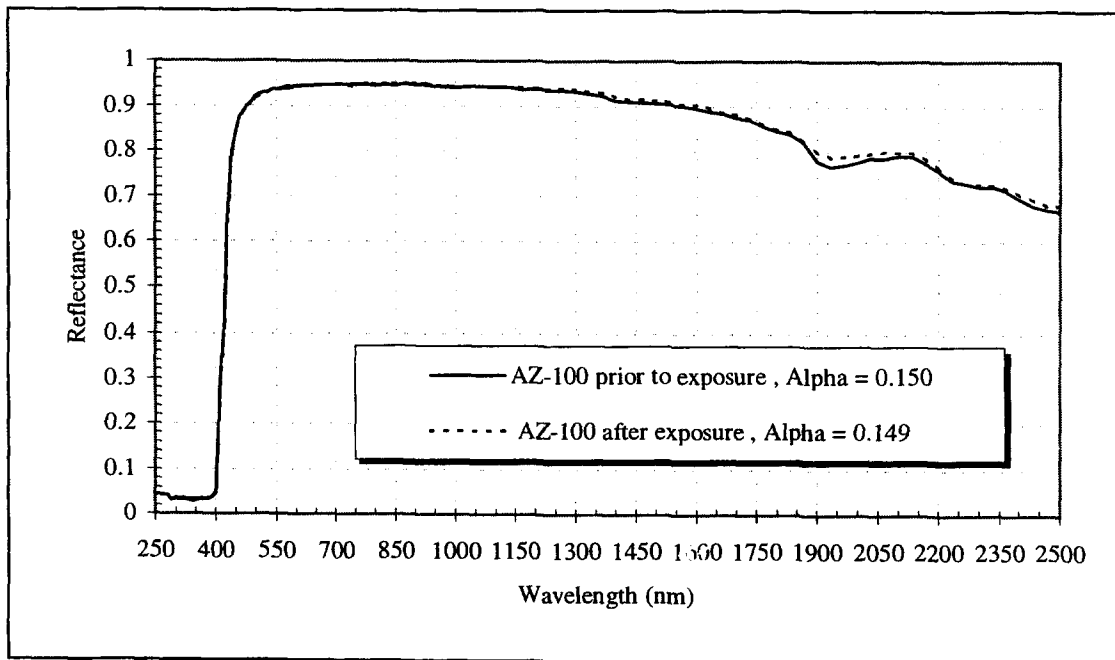


Figure 25. Solar Absorptance of AZ-100

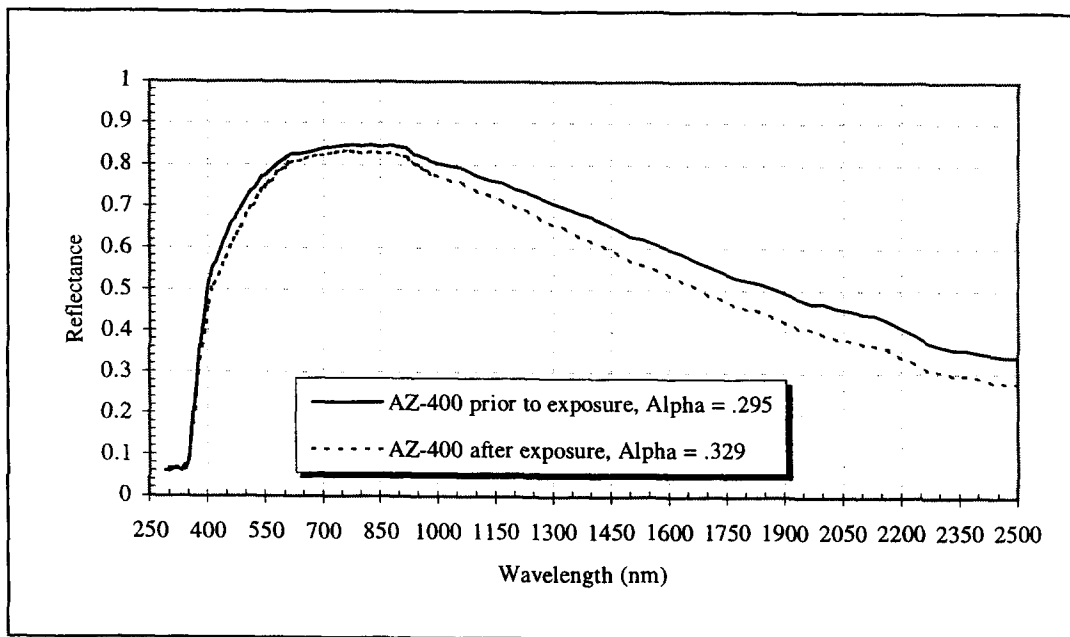


Figure 26. Solar Absorptance of RM-400

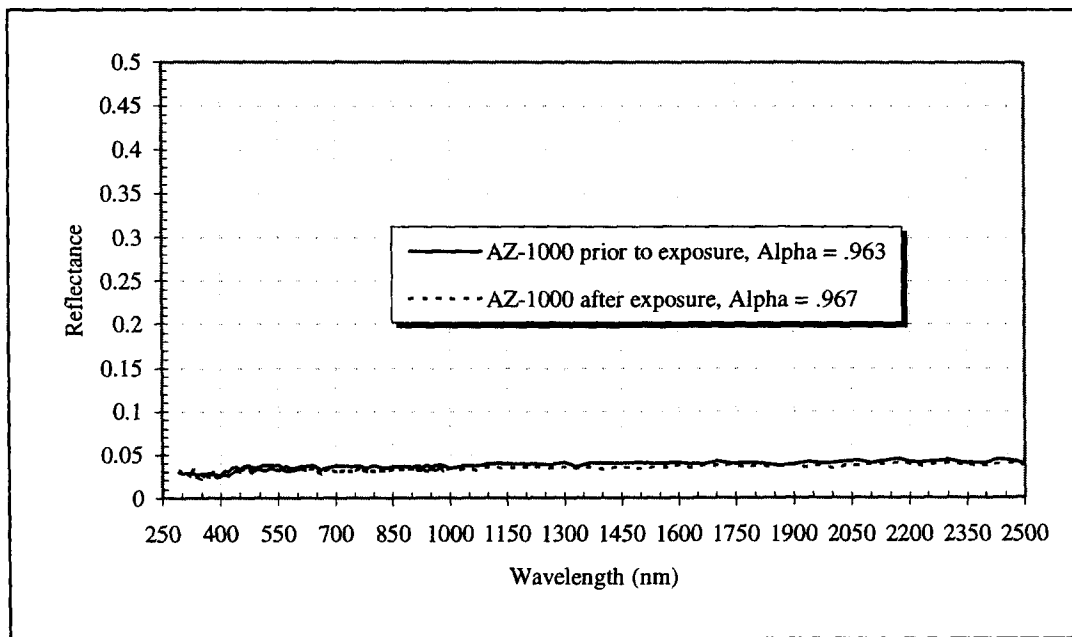


Figure 27. Solar Absorptance of AZ-1000

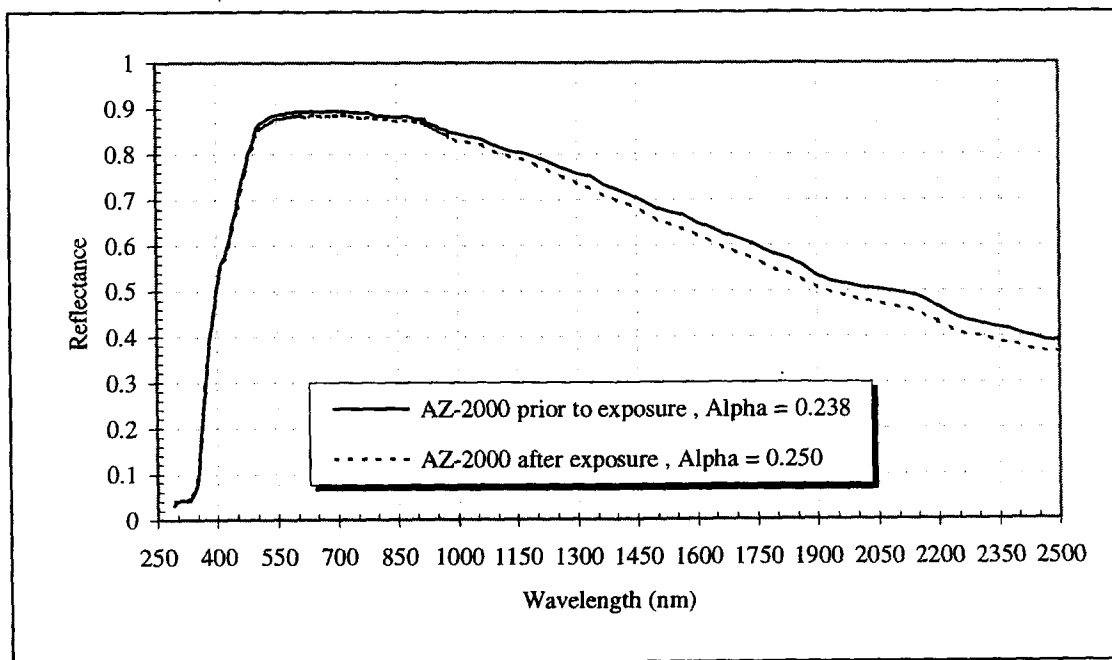


Figure 28. Solar Absorptance of AZ-2000

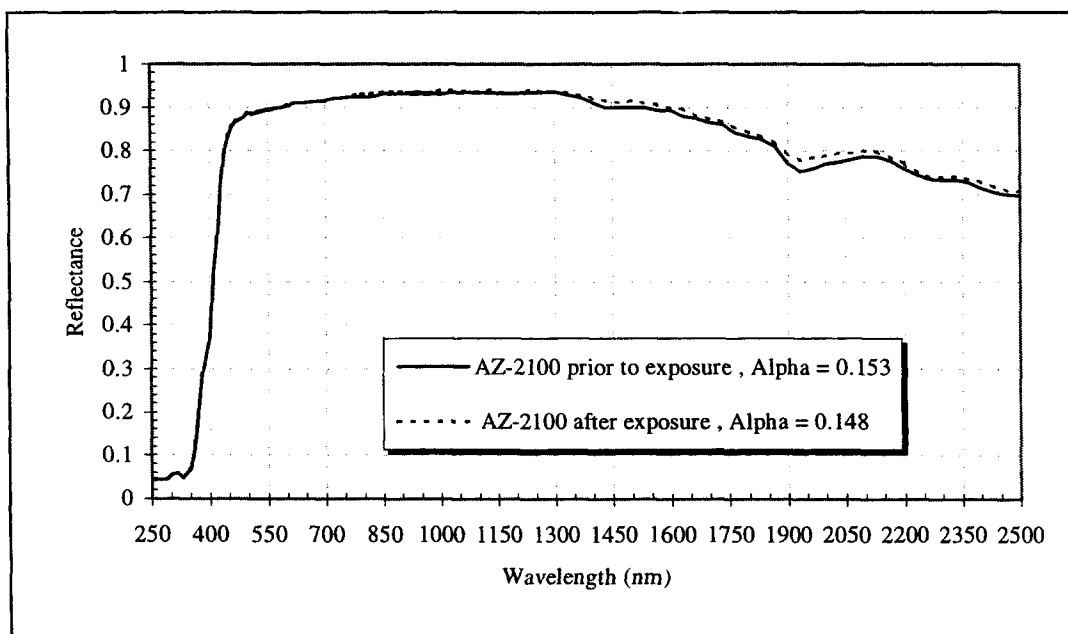


Figure 29. Solar Absorptance of AZ-2100

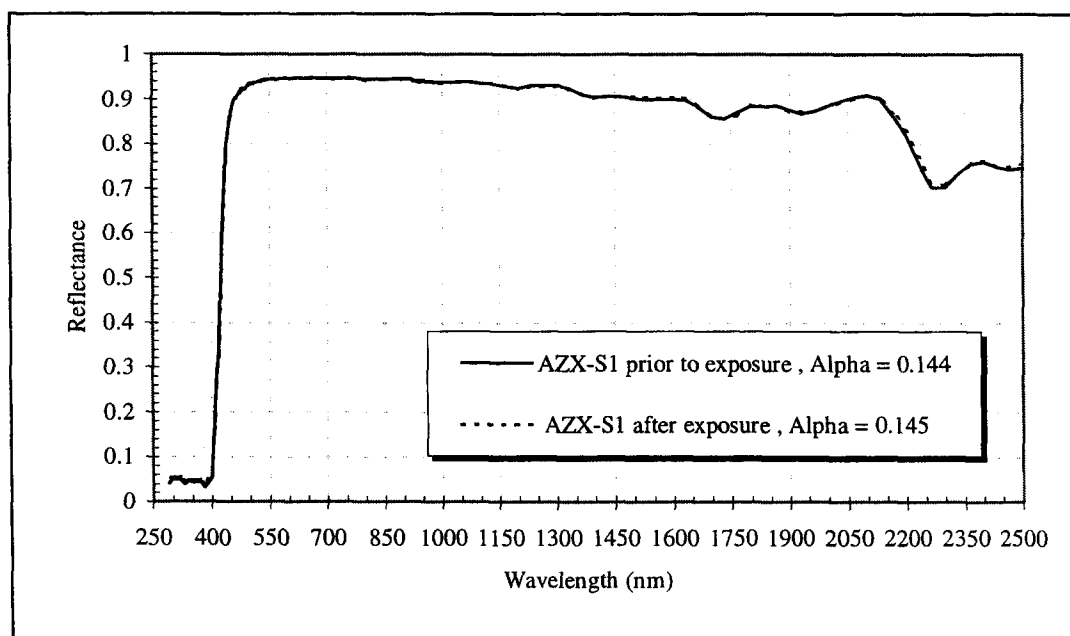


Figure 30. Solar Absorptance of AZX-S1

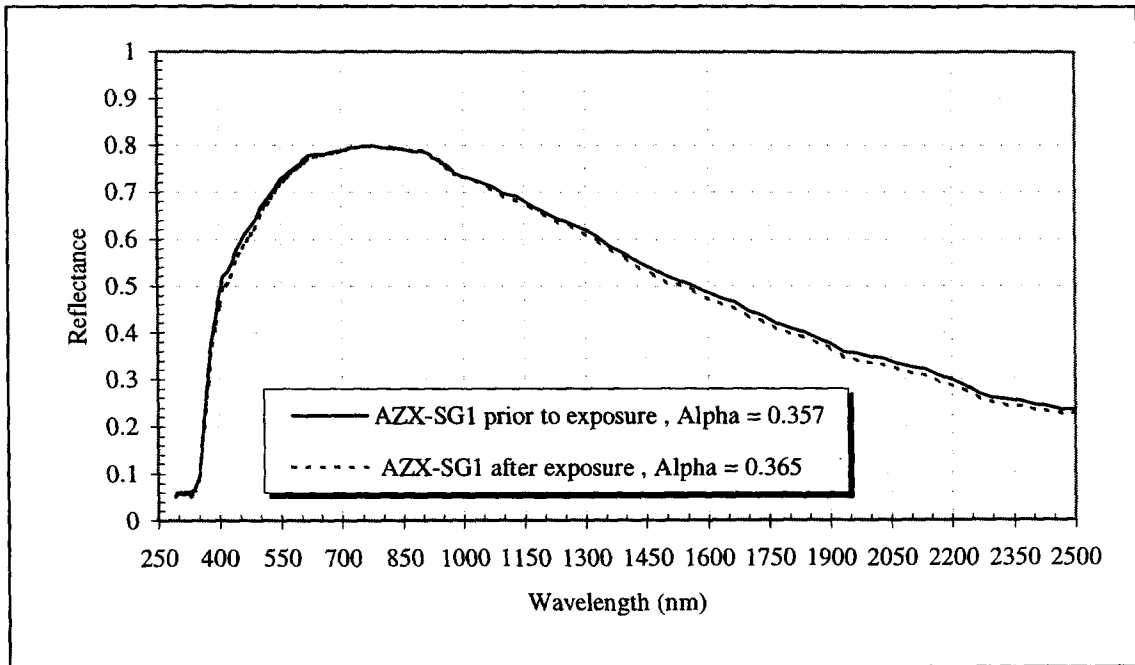


Figure 31. Solar Absorptance of AZX-SG1

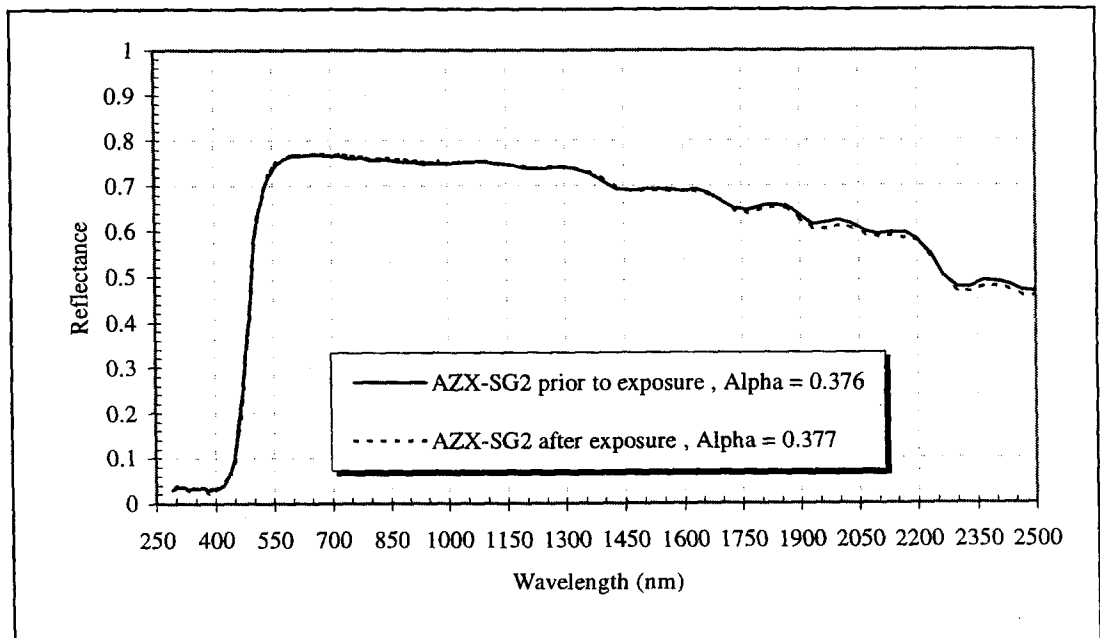


Figure 32. Solar Absorptance of AZX-SG2

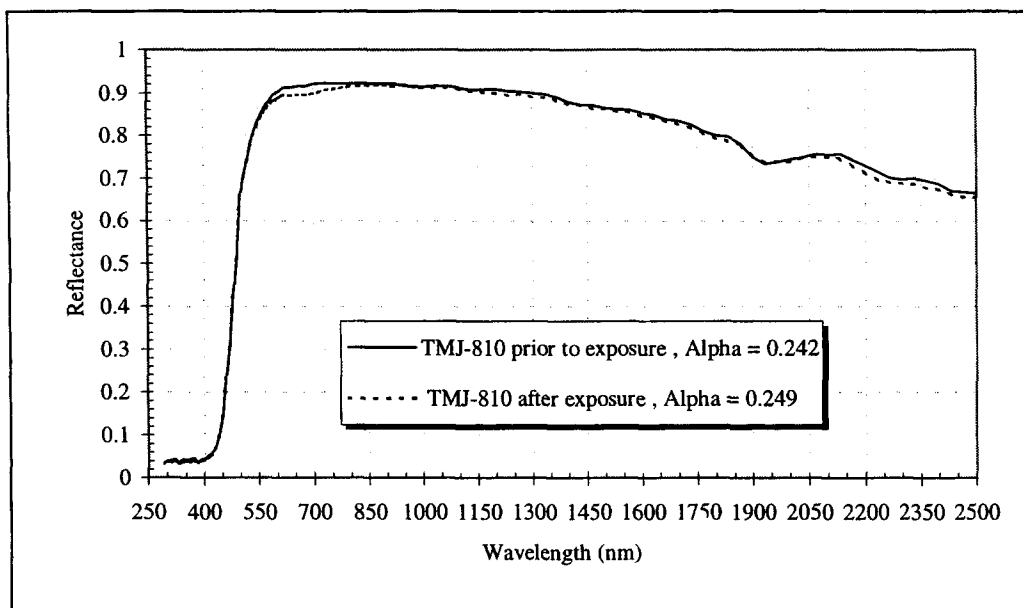


Figure 33. Solar Absorptance of TMJ-810

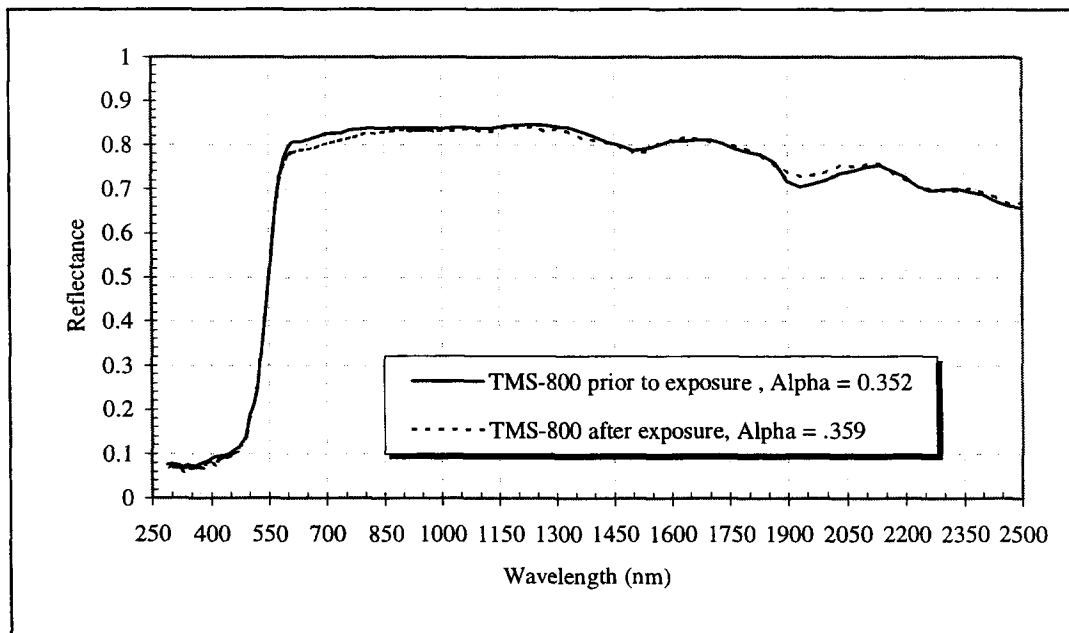


Figure 34. Solar Absorptance of TMS-800

APPENDIX B

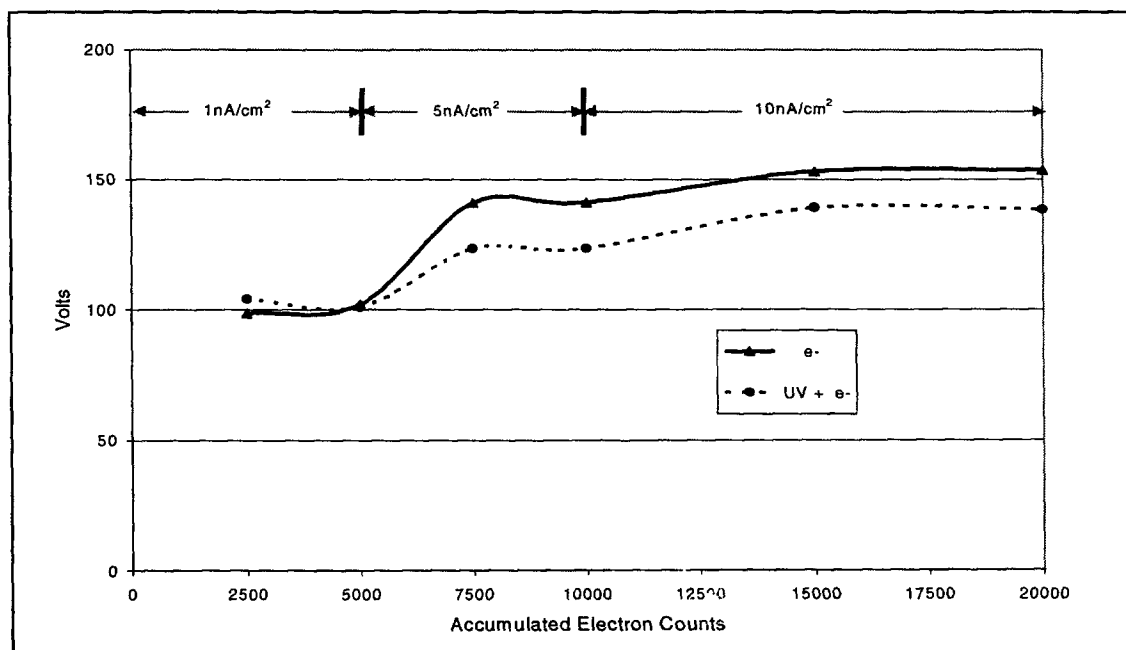


Figure 35. Surface Voltage Measurements of AZ-70

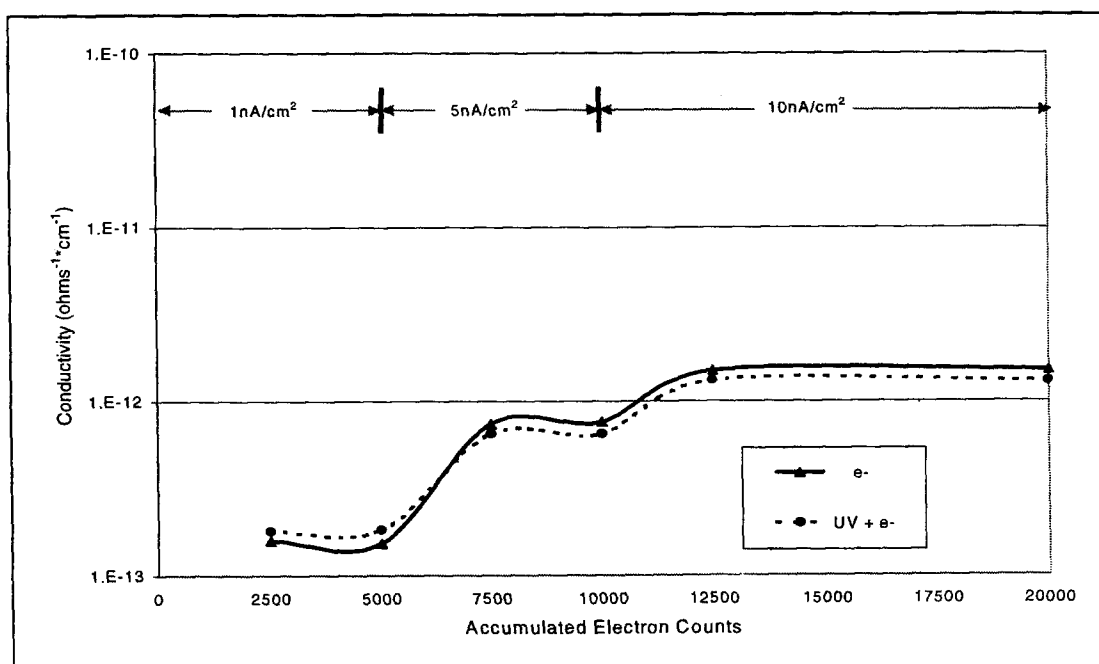


Figure 36. Calculated conductivity values for AZ-70

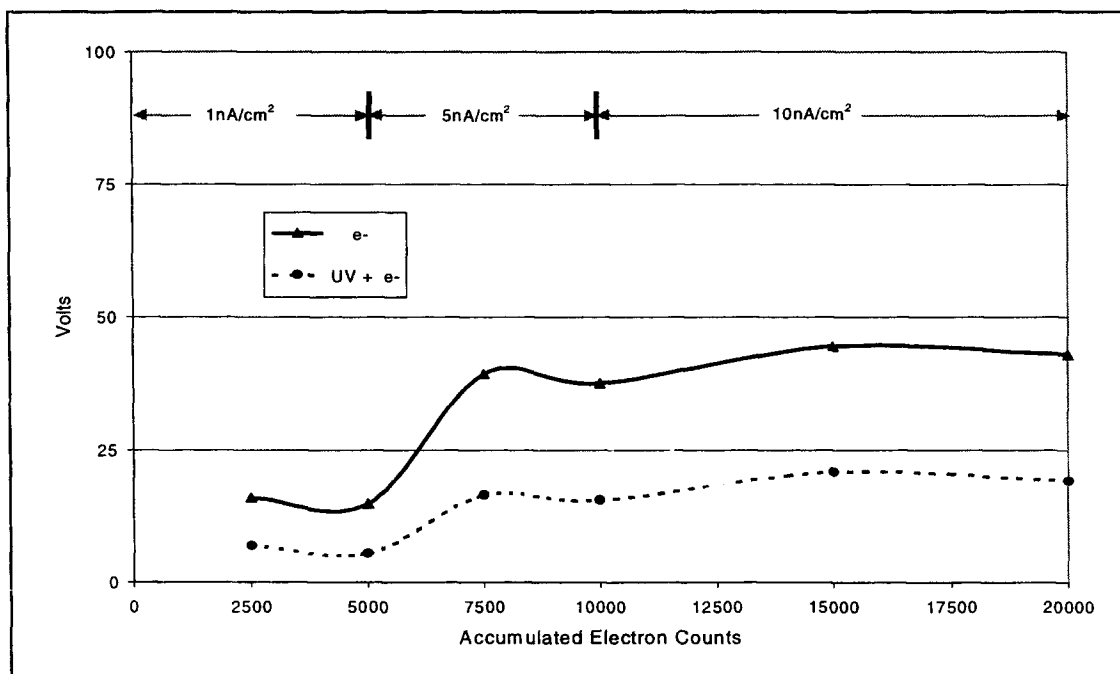


Figure 37. Surface voltage measurements of AZ-93

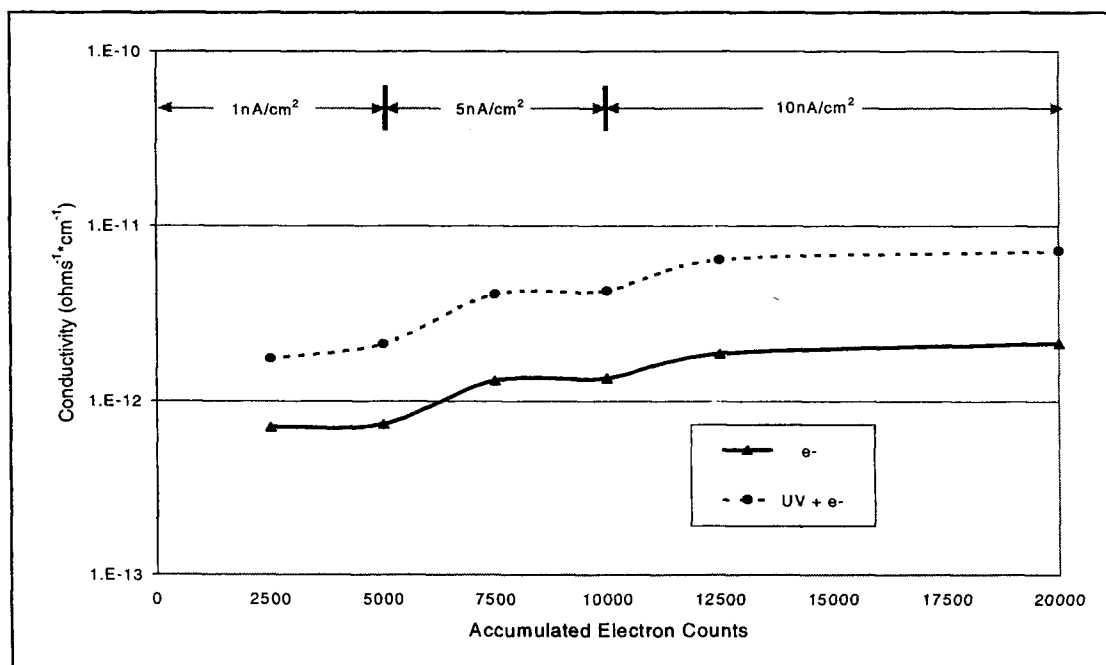


Figure 38. Calculated conductivity values for AZ-93

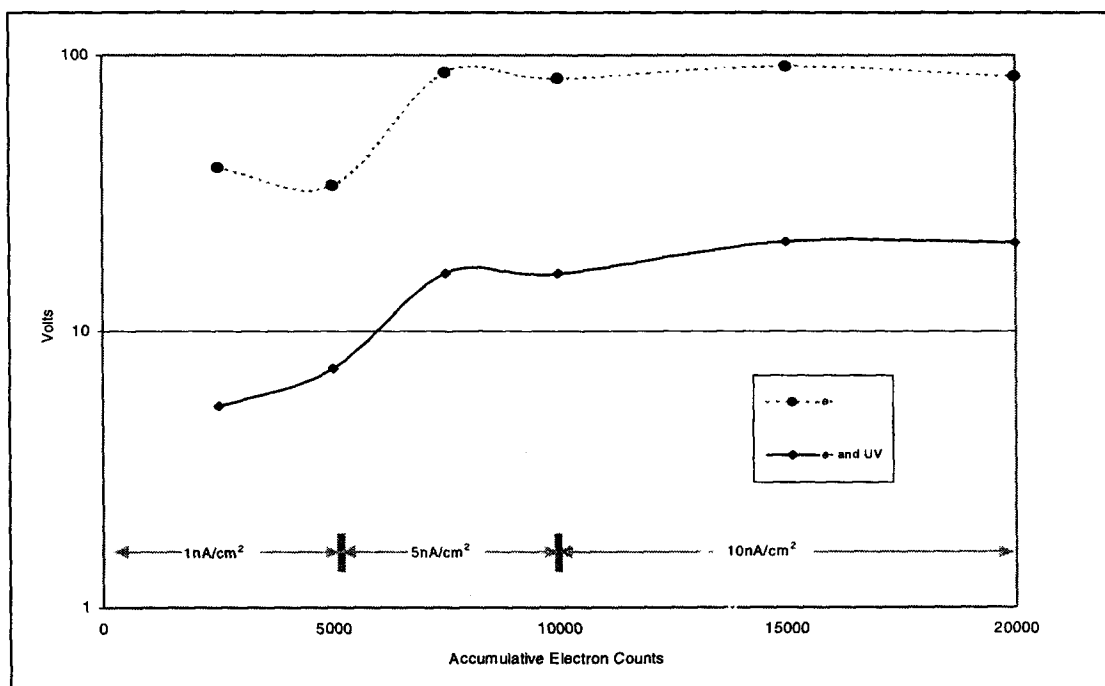


Figure 39. Surface voltage Measurements of AZ-100

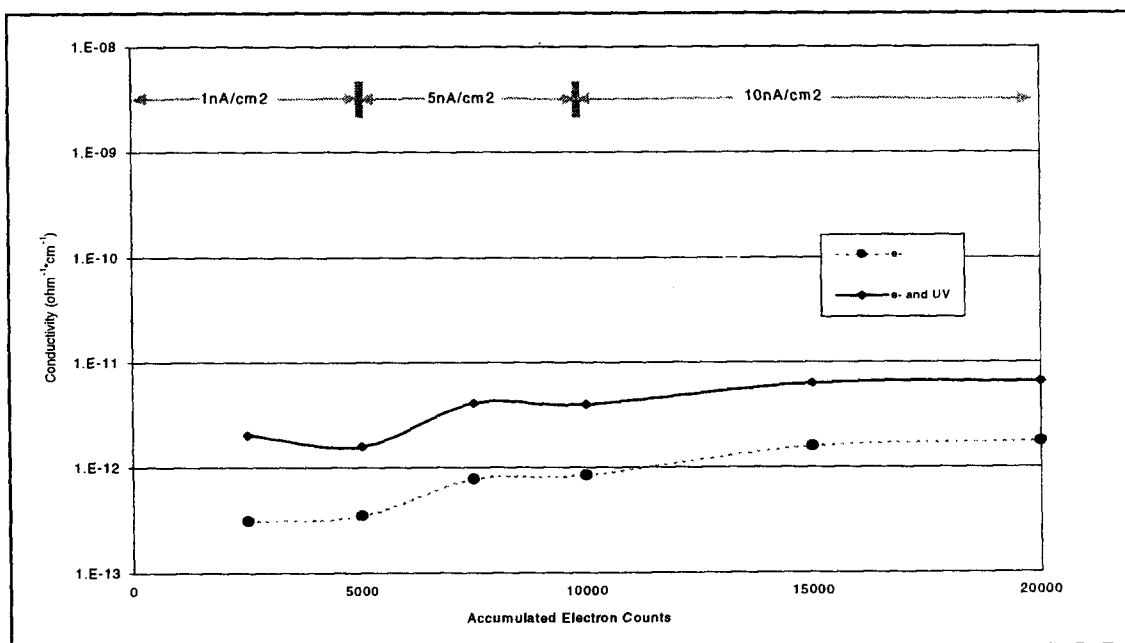


Figure 40. Calculated Conductivity Values for AZ-100

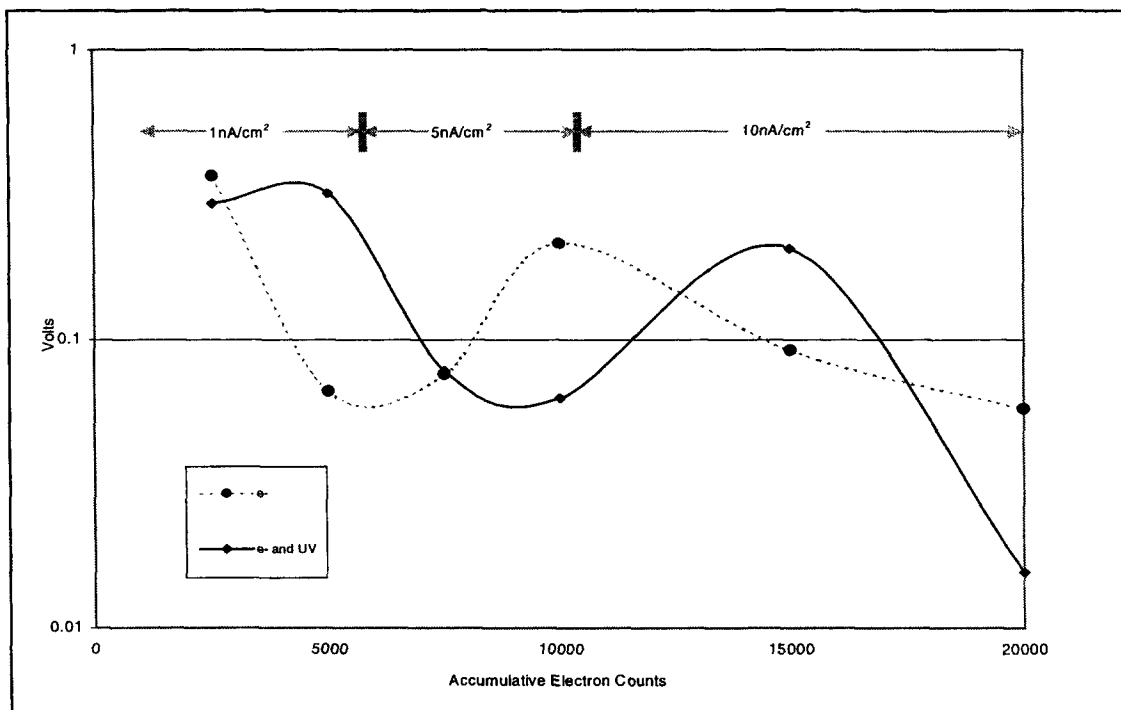


Figure 41. Surface Voltage Measurements of AZ-400

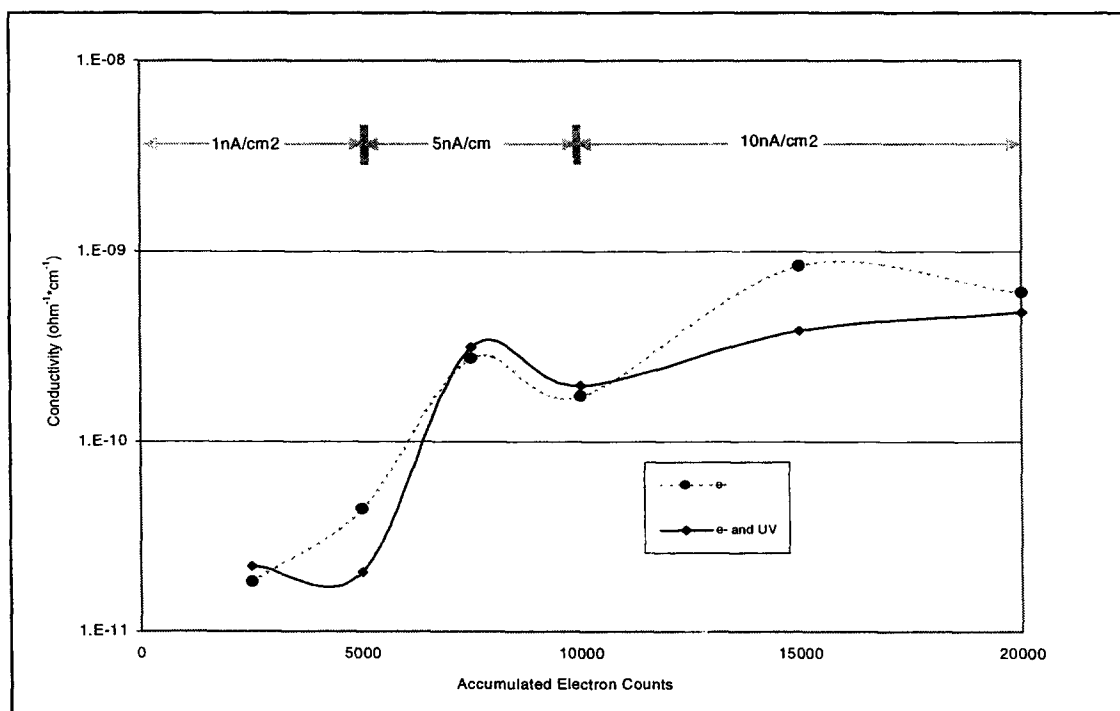


Figure 42. Calculated Conductivity Values for AZ-400

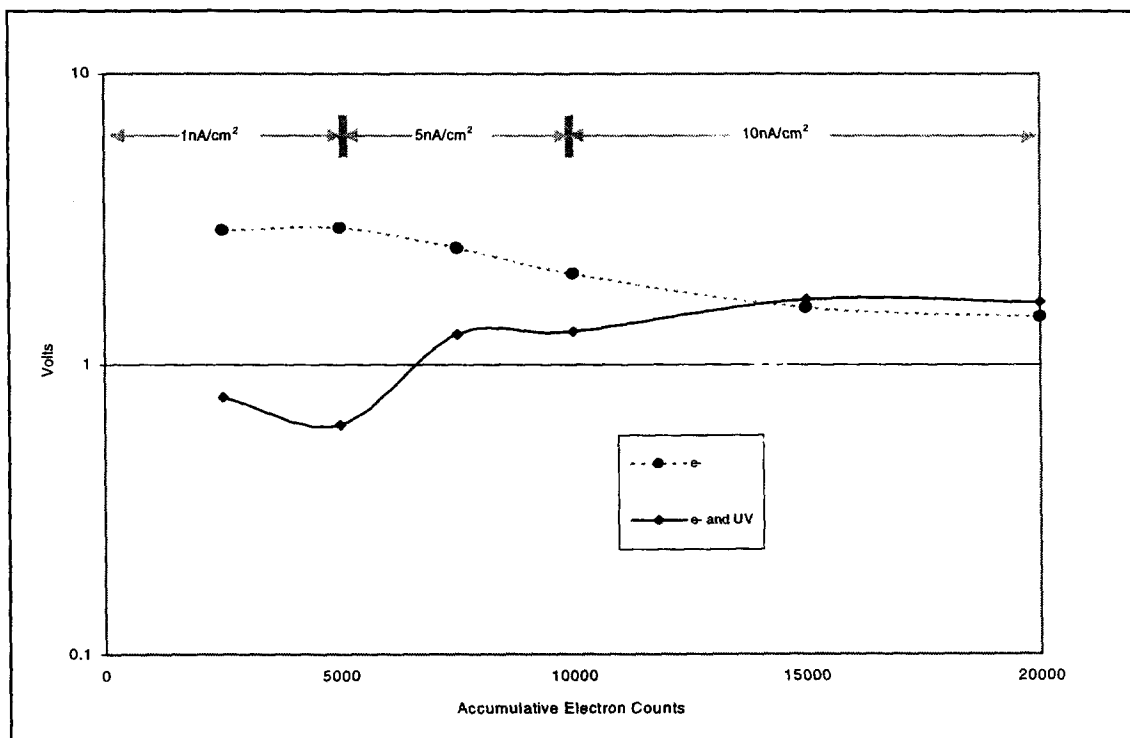


Figure 43. Surface Voltage Measurements of AZ-1000

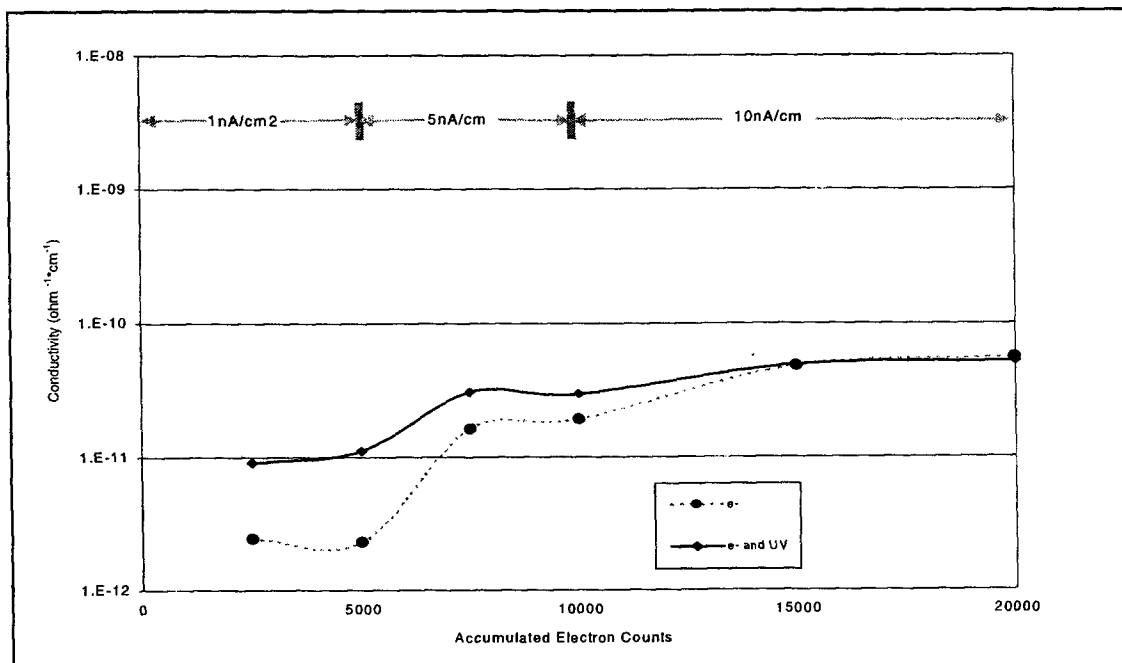


Figure 44. Calculated Conductivity Values for AZ-1000

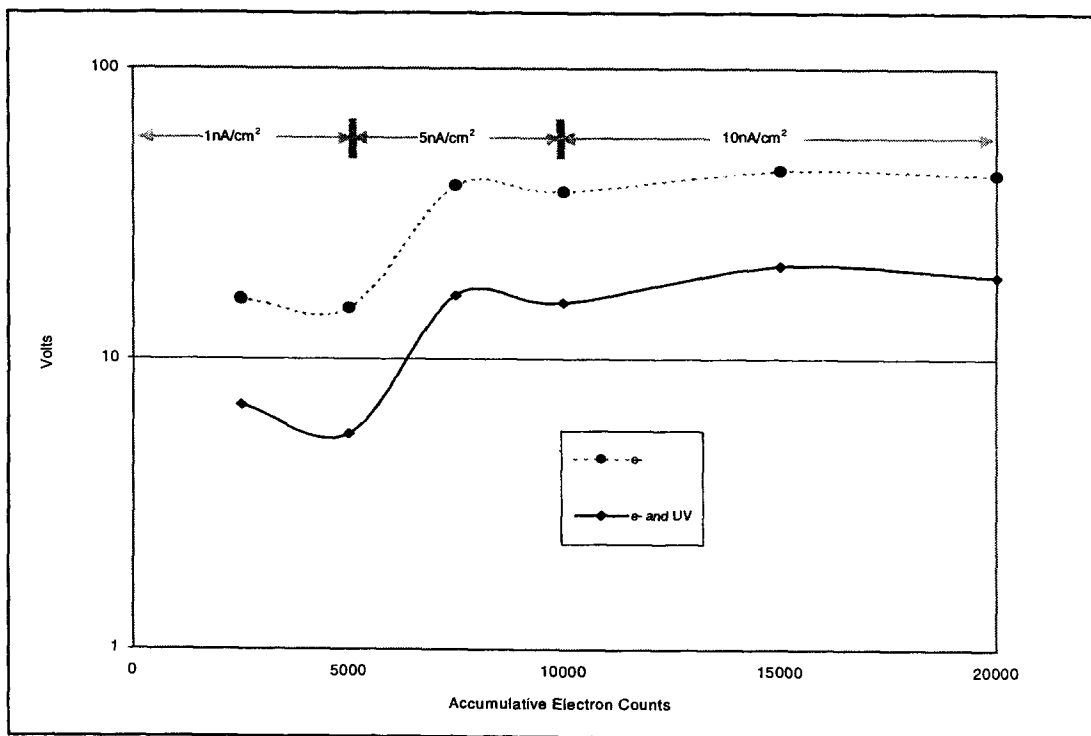


Figure 45. Surface Voltage Measurements of AZ-2000

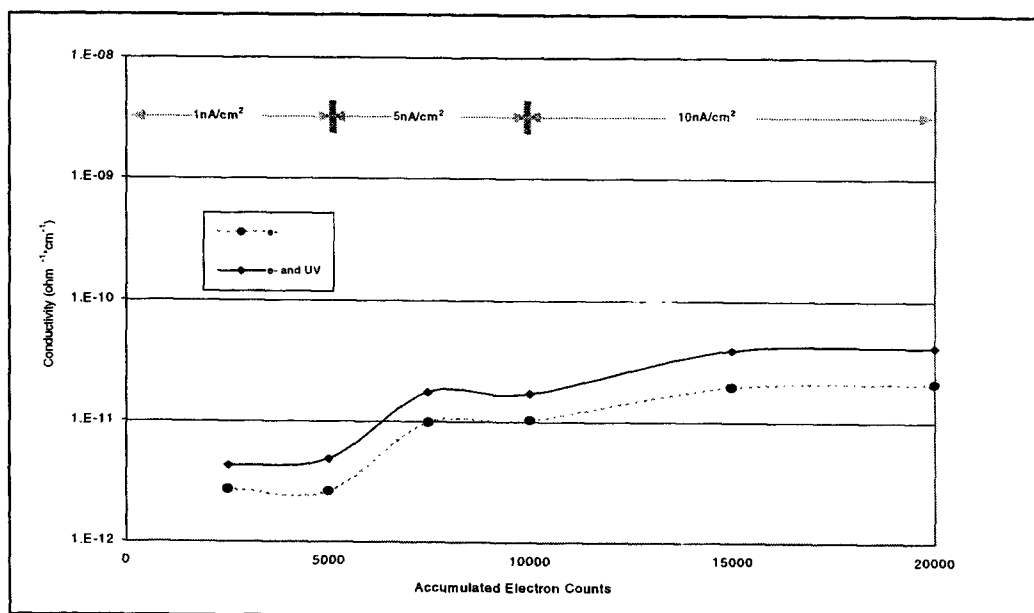


Figure 46. Calculated Conductivity Values for AZ-2000

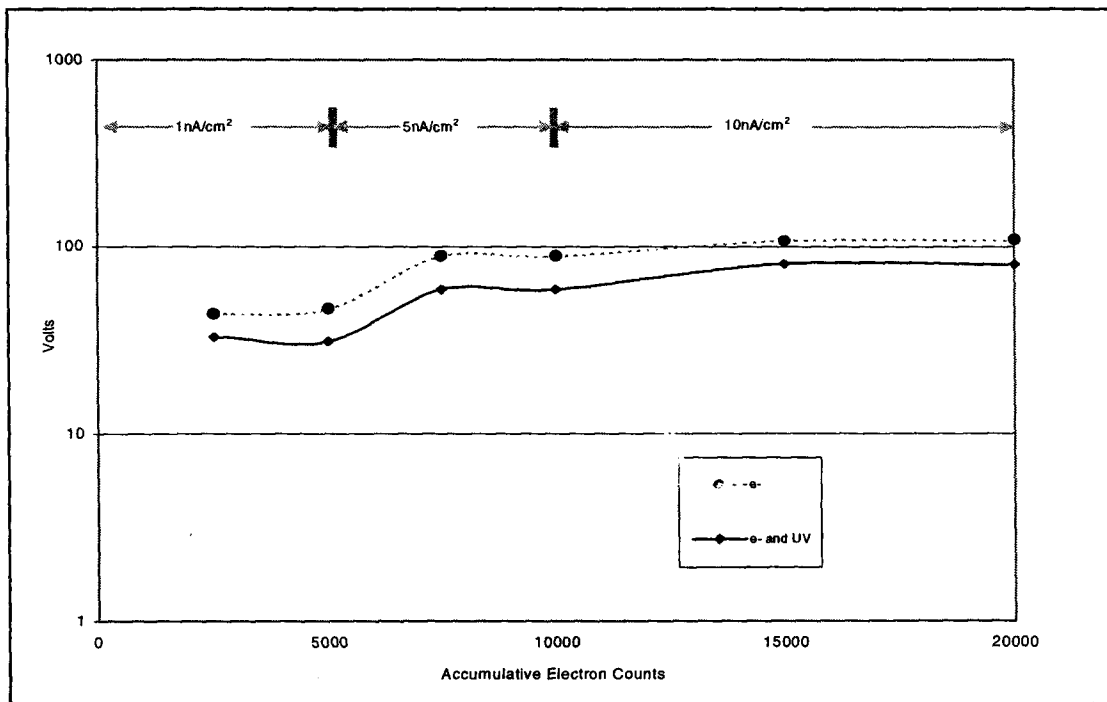


Figure 47. Surface Voltage Measurements of AZ-2100

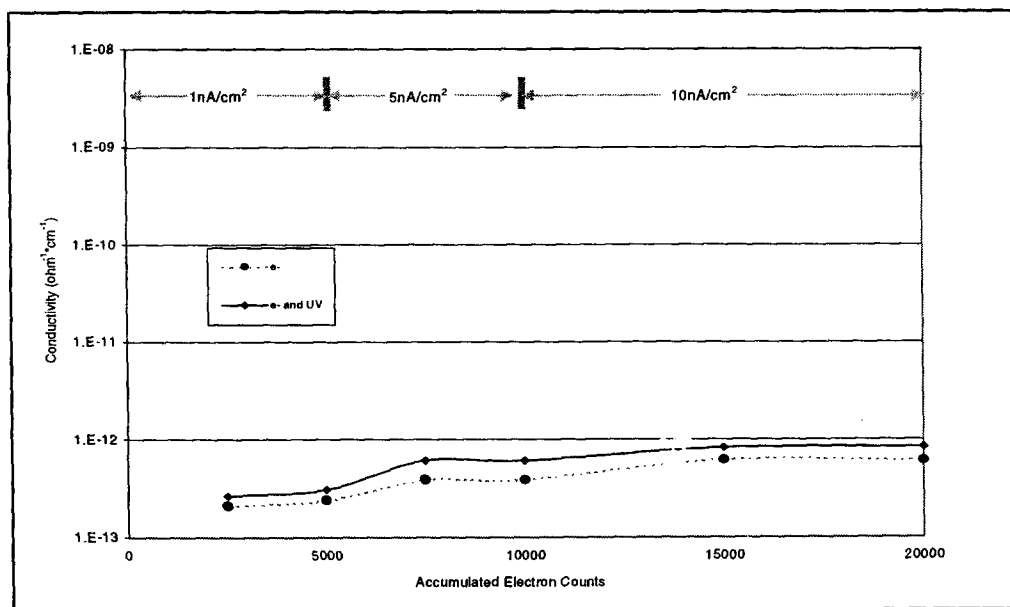


Figure 48. Calculated Conductivity Values for AZ-2100

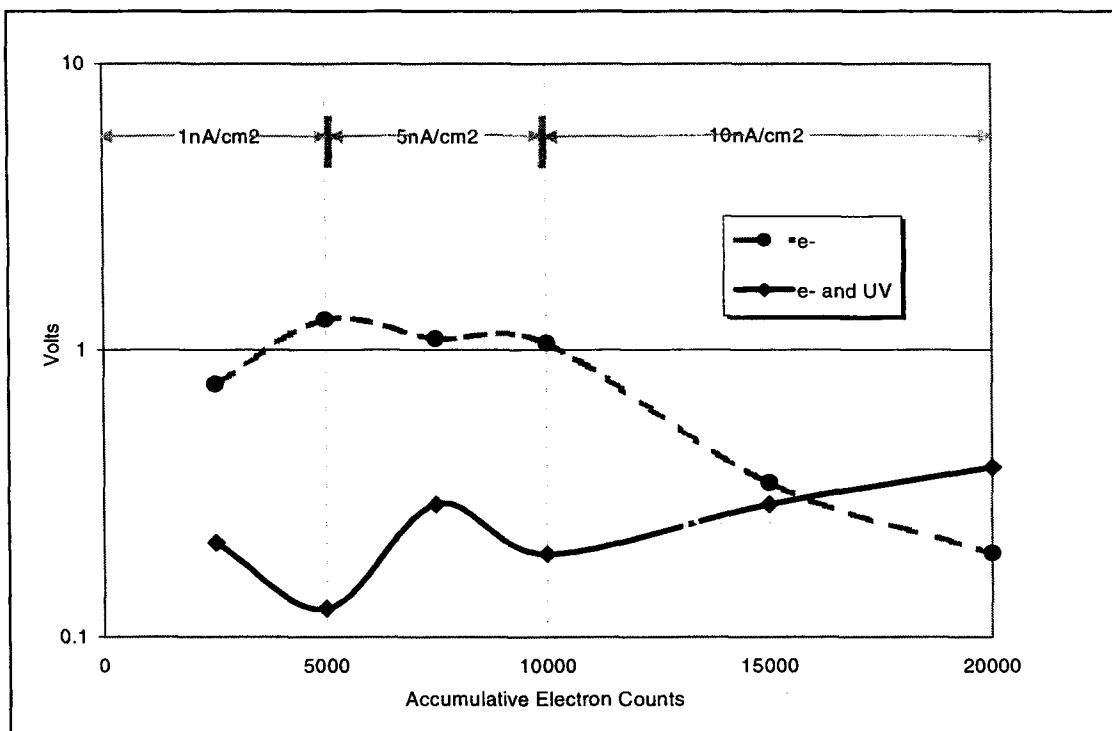


Figure 49. Surface Voltage Measurements of AZX-S1

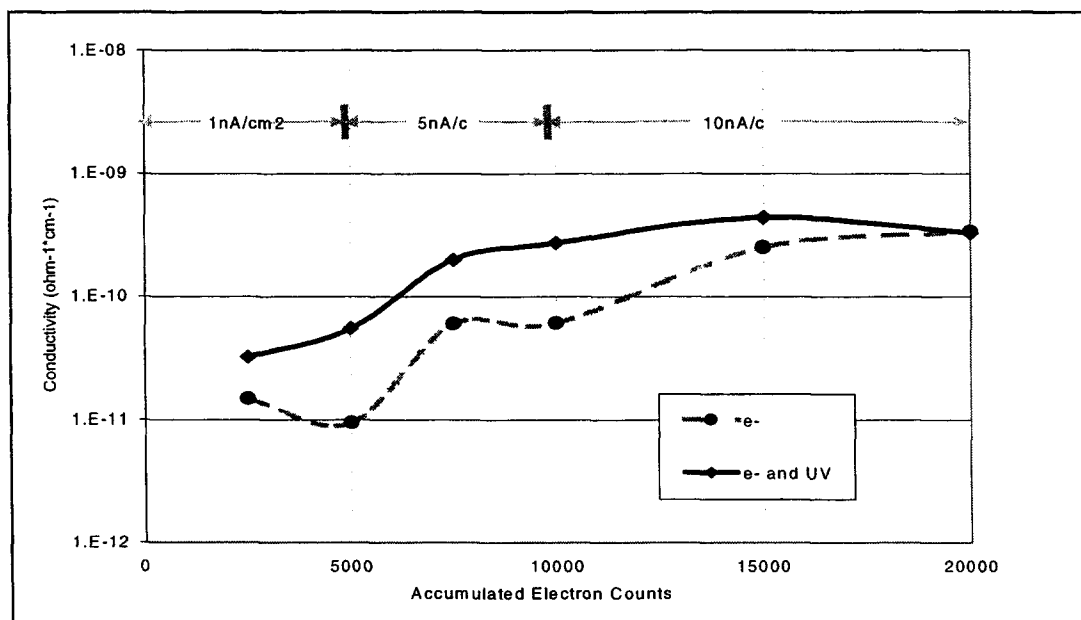


Figure 50. Calculated Conductivity Values for AZX-S1

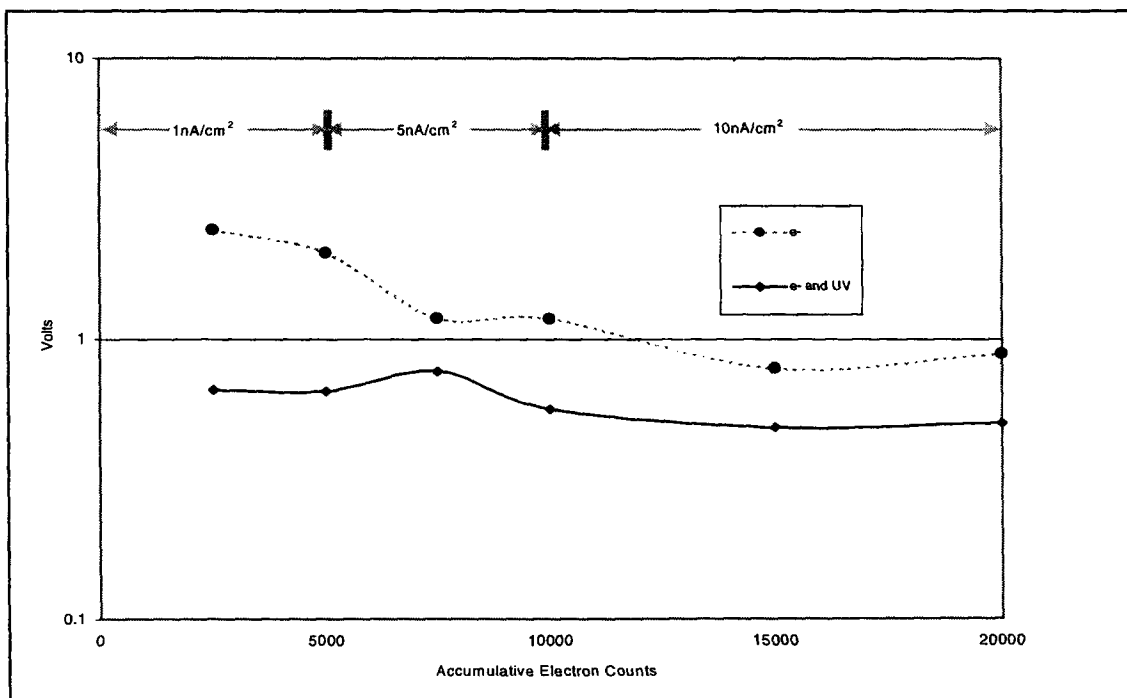


Figure 51. Surface Voltage Measurements of AZX-SG1

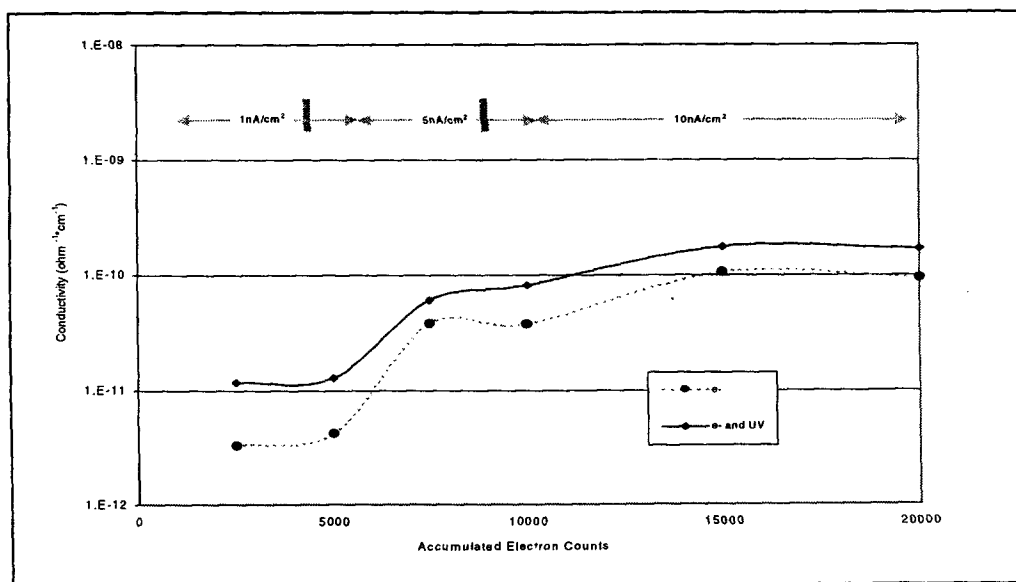


Figure 52. Calculated Conductivity for AZX-SG1

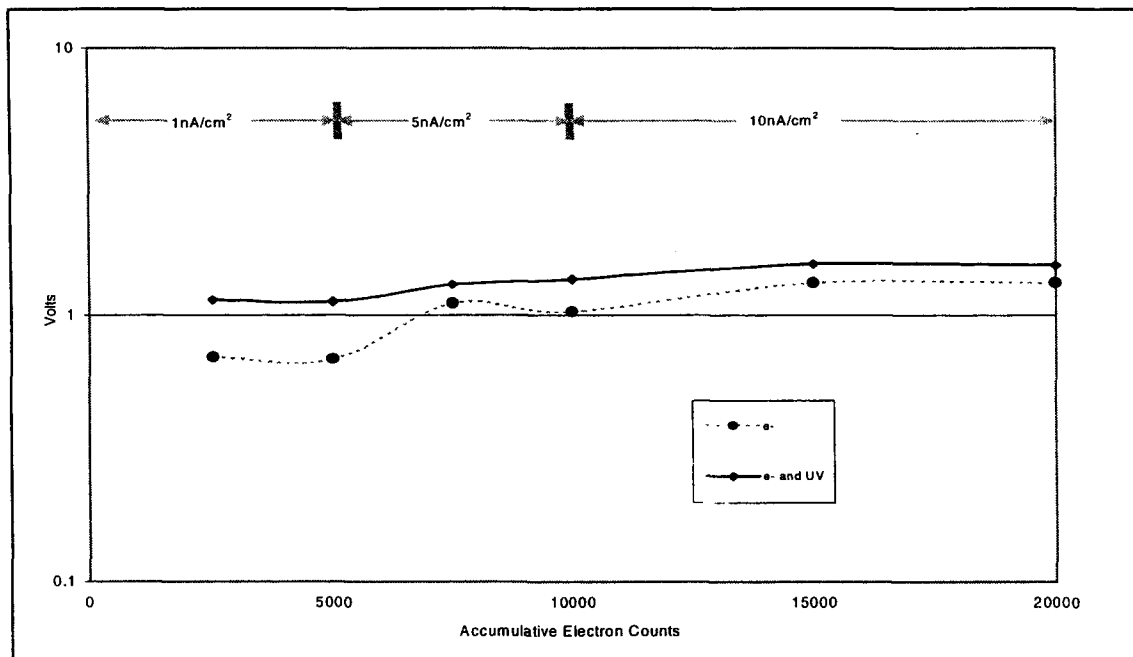


Figure 53. Surface Voltage Measurements of TMJ-810

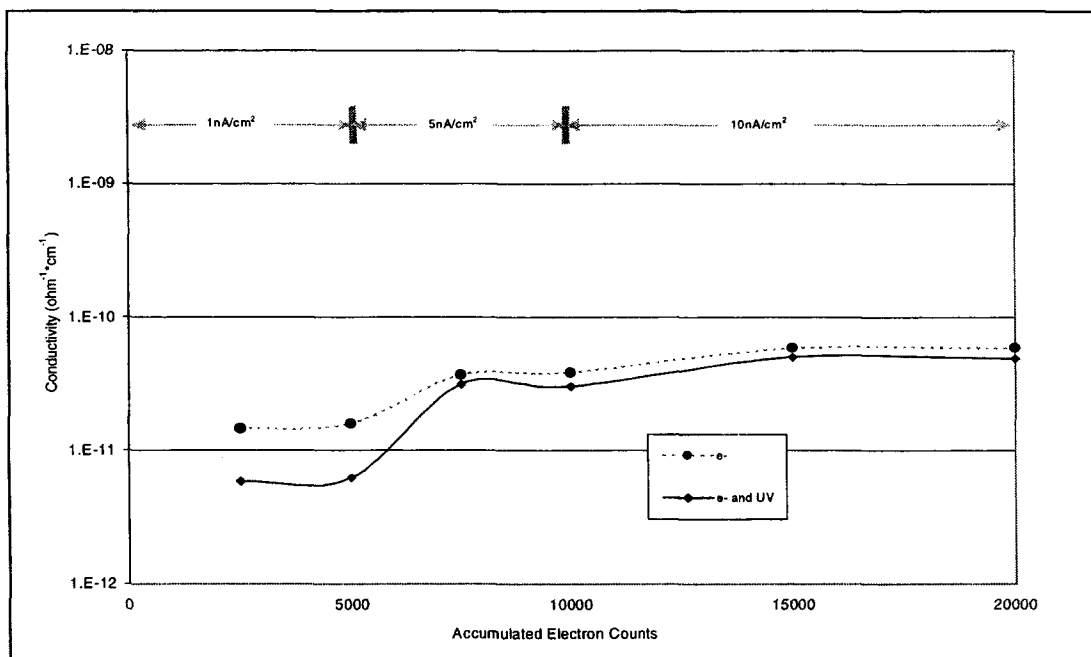


Figure 54. Calculated Conductivity Values for TMJ-810

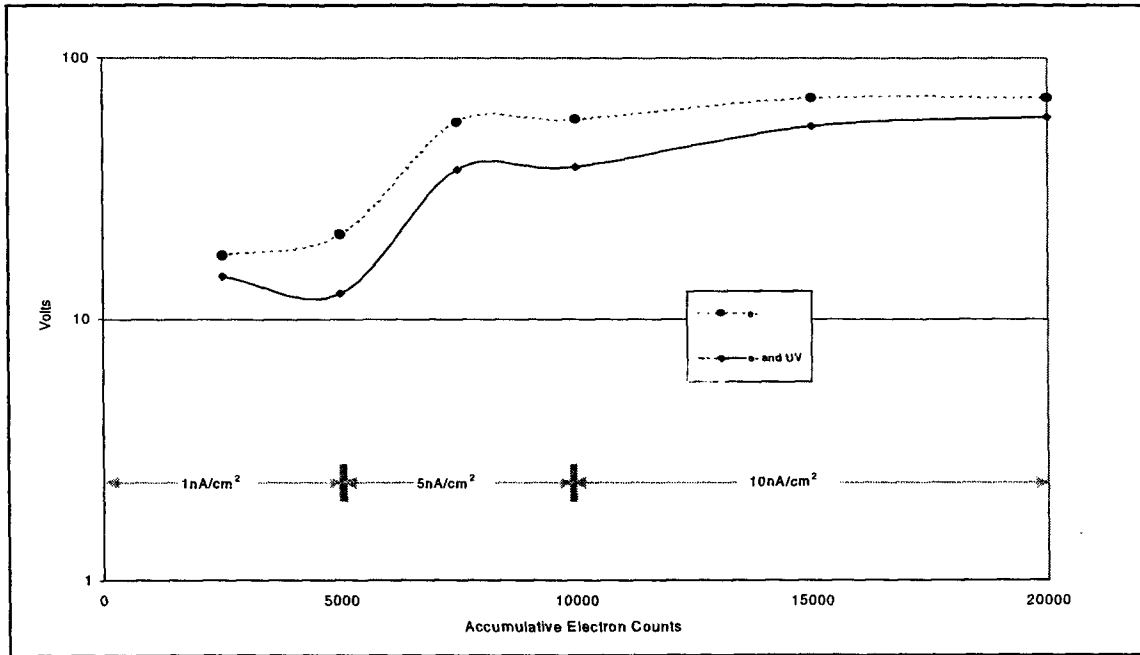


Figure 55. Surface Voltage Measurements of TMS-800

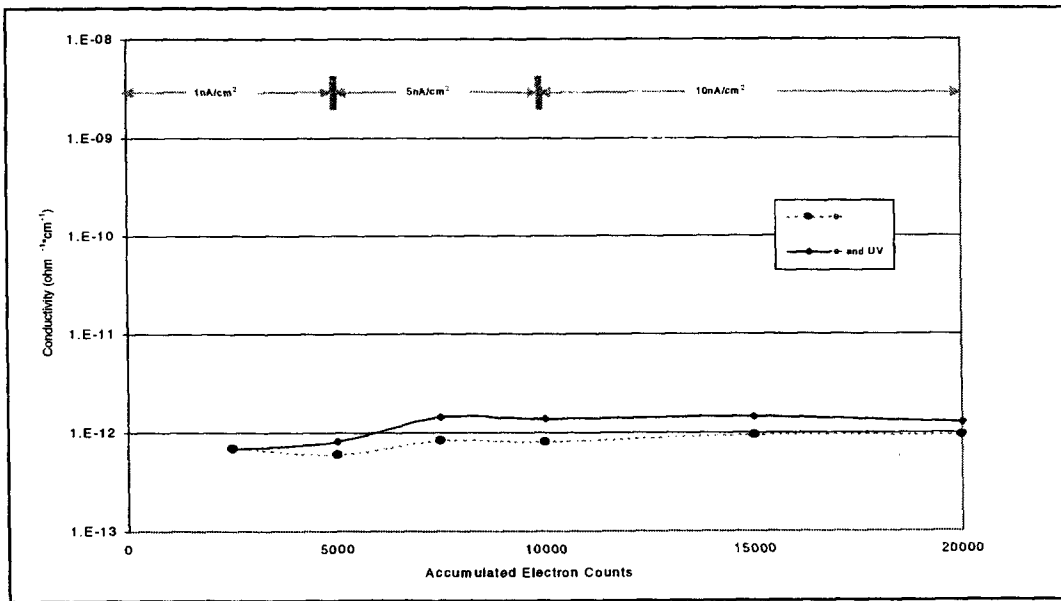


Figure 56. Calculated Conductivity Values for TMS-800

REPORT DOCUMENTATION PAGE			Form Approved OMB No. 0704-0188	
Public reporting burden for this collection of information is estimated to average 1 hour per response, including the time for reviewing instructions, searching existing data sources, gathering and maintaining the data needed, and completing and reviewing the collection of information. Send comments regarding this burden estimate or any other aspect of this collection of information, including suggestions for reducing this burden, to Washington Headquarters Services, Directorate for Information Operation and Reports, 1215 Jefferson Davis Highway, Suite 1204, Arlington, VA 22202-4302, and to the Office of Management and Budget, Paperwork Reduction Project (0704-0188), Washington, DC 20503				
1. AGENCY USE ONLY (Leave Blank)		2. REPORT DATE December 2001		3. REPORT TYPE AND DATES COVERED Contractor Report (Final)
4. TITLE AND SUBTITLE Testing and Optimization of Electrically Conductive Spacecraft Coatings			5. FUNDING NUMBERS NAS8-98212	
6. AUTHORS R.J. Mell* and G.E. Wertz				
7. PERFORMING ORGANIZATION NAMES(S) AND ADDRESS(ES) AZ Technology, Inc. 7047 Old Madison Pike, Suite 300 Huntsville, AL 35806			8. PERFORMING ORGANIZATION REPORT NUMBER M-1035	
9. SPONSORING/MONITORING AGENCY NAME(S) AND ADDRESS(ES) George C. Marshall Space Flight Center Marshall Space Flight Center, AL 35812			10. SPONSORING/MONITORING AGENCY REPORT NUMBER NASA/CR-2001-211411	
11. SUPPLEMENTARY NOTES Prepared for NASA's Space Environments and Effects (SEE) Program *AZ Technology, Inc.; Technical Monitor: D.L. Edwards				
12a. DISTRIBUTION/AVAILABILITY STATEMENT Unclassified-Unlimited Subject Category 88 Standard Distribution			12b. DISTRIBUTION CODE	
13. ABSTRACT (Maximum 200 words) This is the final report discussing the work done for the Space Environments and Effects (SEE) Program. It discusses test chamber design, coating research, and test results on electrically thermal control coatings. These thermal control coatings are being developed to have several orders of magnitude higher electrical conductivity than most available thermal control coatings. Most current coatings tend to have a range in surface resistivity from 1,011 to 1,013 ohms/sq. Historically, spacecraft have had thermal control surfaces composed of dielectric materials of either polymers (paints and metalized films) or glasses (ceramic paints and optical solar reflectors). Very seldom has the thermal control surface of a spacecraft been a metal where the surface would be intrinsically electrically conductive. The poor thermal optical properties of most metals have, in most cases, stopped them from being used as a thermal control surface. Metals low infrared emittance (generally considered poor for thermal control surfaces) and/or solar absorptance, have resulted in the use of various dielectric coatings or films being applied over the substrate materials in order to obtain the required optical properties.				
14. SUBJECT TERMS surface charging, coatings, thermal control			15. NUMBER OF PAGES 60	
			16. PRICE CODE	
17. SECURITY CLASSIFICATION OF REPORT Unclassified	18. SECURITY CLASSIFICATION OF THIS PAGE Unclassified	19. SECURITY CLASSIFICATION OF ABSTRACT Unclassified	20. LIMITATION OF ABSTRACT Unlimited	

National Aeronautics and
Space Administration
AD33

George C. Marshall Space Flight Center
Marshall Space Flight Center, Alabama
35812